SLAC-PUB-3819
October 1985
(T/E)

HADRON SPECTROSCOPY*

Susan Cooper§

Stanford Linear Accelerator Center
Stanford University, Stanford, California 94305

CONTENTS

1. INTRODUCTION

Hadron spectroscopy is a very broad subject, many interesting parts of which have been left out of this talk, in an attempt to discuss a few in a comprehensible manner. I have chosen to emphasize particles which are relevant to testing QCD - heavy quark systems and glueball candidates.

*Work supported by the Department of Energy, contract DE-AC03-76SF00515.
§Mailing address: DESY, Notkestraße 85, D-2000 Hamburg 52, W. Germany

Extended version of Rapporteur talk given at the International Europhysics Conference on High Energy Physics, Bari, Italy, July 18-24, 1985.

The talk is organized in order of decreasing quark mass, starting at the easy end: the heaviest spectroscopically observed quarks, $b\bar{b}$, form bound states which are quite well behaved. Results from four experiments on the χ_b ($1\,^3P_J$ $b\bar{b}$) states are now final and need only brief discussion. New results on the χ_c states from the ISR are also presented. The χ state masses, spins, and hadronic widths fit well into the picture provided by the non-relativistic potential models and, to the extent it can currently be applied to bound states, by QCD.

In section 3 other heavy states are discussed. Heavy quarks combined with light ones yield the recently observed B^* and F^*, which appear exactly where expected by simple extrapolation from lighter-quark vector mesons. A D^{**}, and perhaps an Ω^*, have also been observed.

Radiative Υ and J/ψ decays respectively had previously yielded evidence for two unexplained particles, the $\varsigma(8.3)$ and the $\xi(2.2)$. Their status in light of new data is briefly reviewed, along with upper limits for Higgs and η_b production.

Sections 4, 5, and 6 are devoted to the gluonium candidates $\iota(1460)$, $\Theta(1700)$, and $g_T(\sim 2200)$. The first two of these were discovered in radiative J/ψ decays, the third in hadronic production of $\phi\phi$; both of these are supposed to be channels that favor gluonium production. This year the ι may have acquired new decay channels $\rho\rho$ and $\omega\omega$. But the biggest news on the ι actually comes from the E(1420). It has been regarded as a 1^{++} meson for several years. Now new data indicates 0^{-+}, re-opening the possibility of the E and ι being the same particle. There is tentative evidence for both Θ and ι production in hadronic reactions which, if substantiated, may help us learn more about glueball formation. A glueball should have SU(3) symmetric decays, but search for a $\pi\pi$ decay of the Θ is proving difficult. New experiments on $\phi\phi$ confirm the 2^{++} character of the threshold region, but do not have the analysing power to confirm the existence of three resonances in this channel.

Section 7 addresses the very lightest $q\bar{q}$ mesons, the π^0 and η. Recent total width measurements from two photon production agree well with a new distance-of-flight measurement of the π^0 lifetime, but disagree significantly with the previous Primakoff-effect measurement of the η lifetime.

2. THE χ STATES

The bound states of charm quarks have been a useful laboratory for studying the inter-quark force. The question of flavor-independence of the inter-quark force, along with the relatively large relativistic corrections in the $c\bar{c}$ system ($v/c \sim 1/2$), lead to heightened interest in the study of the $b\bar{b}$ system. even though it is considerably more difficult experimentally due to lower event rates and higher background.

Table I lists the expected $b\bar{b}$ states. The Υ's, produced directly in e^+e^- annihilation, are well known, and fit astoundingly well the spectrum expected from the $c\bar{c}$ system when adjusted for the mass of the b quark. The χ_b' and χ_b states, which can be reached by photon transitions from the Υ'' and Υ', were first observed by CUSB in 1982 and 1983[1,2]; they plan to take more data next year to improve the χ_b' results. Since these states have different orbital angular

Table I. Expected $b\bar{b}$ states below threshold for B meson production

The states are listed in order of increasing mass, except for the $^1P_1$, which is expected to be near the $^3P_{cog}$. The spectroscopic notation is n $^{2S+1}L_J$; S is the total spin of the quarks, L their relative angular momentum, and J the total angular momentum; n=1 for the lowest radial eigenstate of each L, n=2 for the first radial excitation, etc.

	Spectroscopic notation	J^{PC}	Detected	Production in e^+e^-	Dominant decay
η_b	$1\,^1S_0$	0^{-+}		$\hat{\eta}_b \to \gamma\eta_b$, $\Upsilon,\Upsilon',\Upsilon'' \to \gamma\eta_b$	gg
Υ	$1\,^3S_1$	1^{--}	yes	$e^+e^- \to \Upsilon$	ggg
χ_b	$1\,^3P_0$	0^{++}	yes	$\Upsilon' \to \gamma\chi_b$	gg
"	$1\,^3P_1$	1^{++}	yes	"	$q\bar{q}g$
"	$1\,^3P_2$	2^{++}	yes	"	gg
$\hat{\eta}_b$	$1\,^1P_1$	1^{+-}		$\Upsilon'' \to \pi\pi\hat{\eta}_b$	ggg, $q\bar{q}g$
η_b'	$2\,^1S_0$	0^{-+}		$\Upsilon',\Upsilon'' \to \gamma\eta_b'$	
Υ'	$2\,^3S_1$	1^{--}	yes	$e^+e^- \to \Upsilon'$	
χ_b'	$2\,^3P_J$	$2^{++},1^{++},0^{++}$	yes	$\Upsilon'' \to \gamma\chi_b'$	
$\hat{\eta}_b'$	$2\,^1P_1$	1^{+-}			
η_b''	$3\,^1S_0$	0^{-+}		$\Upsilon'' \to \gamma\eta_b''$	
Υ''	$3\,^3S_1$	1^{--}	yes	$e^+e^- \to \Upsilon''$	

momentum and spins than the Υ's, measuring their masses yields information on the spin dependent forces.

2.1 MEASUREMENTS OF χ_b MASSES

The ARGUS[3], CLEO[4], Crystal Ball[5] and CUSB[2] collaborations have now analyzed approximately equivalent amounts of $\Upsilon' \to \gamma\chi_b$ data, obtained at the e^+e^- storage rings CESR and DORIS. Preliminary results presented in 1983 and 1984 showed good agreement between all four experiments on the positions of the first two transition photon lines at 109 and 129 MeV, but varied between 149 and 160 MeV on the position of the third line, which is a weaker signal. For this conference, the ARGUS and Crystal Ball groups are able to present their final Υ' inclusive photon spectra[3,5], in which the third line reaches for the first time a significance $> 4\sigma$, and appears at an energy of 163 MeV.

CUSB and Crystal Ball both measure photon energies in NaI(Tl) crystal arrays, and obtain energy resolutions of 7 and 9 MeV respectively at 160 MeV and efficiencies of about 15%. These detectors can observe the χ_b states in both the **inclusive** photon spectrum from $\Upsilon' \to \gamma\chi_b$, $\chi_b \to$ anything; and the

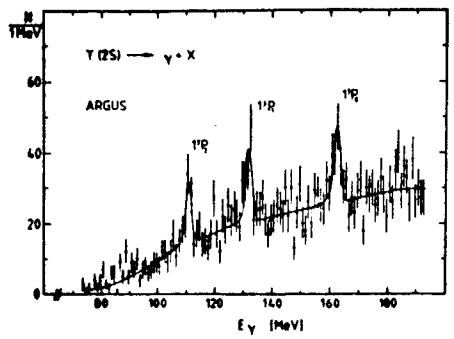

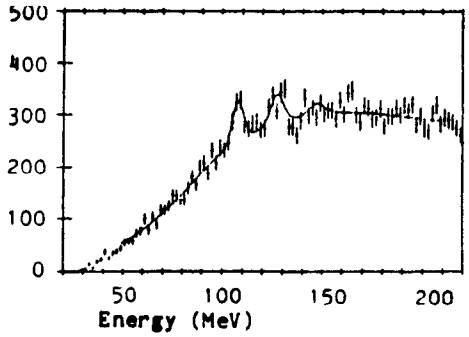

Figure 1. ARGUS $\Upsilon' \to \gamma$+hadrons[3]. The analysis has been improved over that shown last year by using a 5C fit (γ has zero mass, points to primary vertex, conversion vertex is at radius of material). Their excellent resolution (1.1 MeV) allows them to determine that the lines are not Doppler broadened, and thus not from $\chi_b \to \gamma\Upsilon$.

Figure 2. CLEO $\Upsilon' \to \gamma$+hadrons[4]. The spectrum is from a re-analysis performed this year to remove γ's from π^0decays. The data is not sufficient to measure the position of the third line. In the fit shown, it was fixed at the CUSB value.

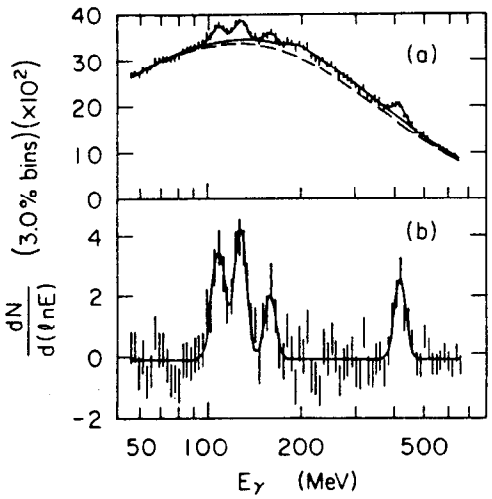

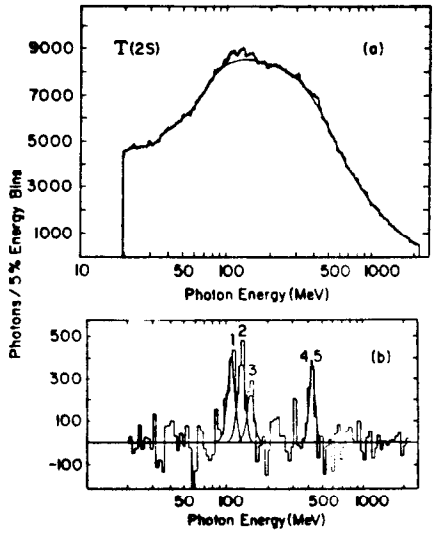

Figure 3. Crystal Ball $\Upsilon' \to \gamma$+hadrons[5]. The broad peak near 210 MeV is due to unidentified minimum-ionizing charged particles; its shape has been determined from particles identified as charged by the inner proportional chambers. This peak causes some uncertainty in the fit, especially for the line at 164 MeV, but careful study has allowed the systematic error on the energy of this line to be reduced to 2.7 MeV. The line at ~400 MeV is from $\chi_b \to \gamma\Upsilon$.

Figure 4. CUSB $\Upsilon' \to \gamma$ + hadrons[2]. The observed spectrum (a) was fit from 65 to 280 MeV with a cubic polynomial background plus 3 Gaussians of width σ/E=6%. The confidence level of this fit is 30%; omitting the third line gives $< 1\%$. The resolution, determined by Monte Carlo, has been checked with π^0's and the $\chi_b \to \gamma\Upsilon$ line in this spectrum at ~400 MeV. Spectrum (b) has the background subtracted.

Table II. Measurements of χ_b states.

χ_b masses and branching ratios from the reactions $\Upsilon' \to \gamma\chi_b$ and $\chi_b \to \gamma\Upsilon$. Masses are in MeV, branching ratios in %.

	ARGUS[3]	CLEO[4]	Crystal Ball[5]	CUSB[2]
$E_\gamma(\Upsilon' \to \gamma\chi_b)$				
$1\,^3P_2$				
inclusive	110.6±.3±0.9	109.0±.6±0.4	110.4±0.8±2.2	108.2±0.3±2
exclusive			107.0±1.1±1.3	$107^{+2.0}_{-2.5} \pm 2$
average			108.2±1.6	107.8±1.7
$1\,^3P_1$				
inclusive	131.7±.3±1.1	128.6±.9±0.4	130.6±0.8±2.4	128.1±0.4±3
exclusive			131.7±0.9±1.3	128.0±1.5±2
average			131.4±1.5	128.0±1.9
$1\,^3P_0$				
inclusive	162.1±0.5±1.4		163.8±1.6±2.7	149.4±0.7±5
$B(\Upsilon' \to \gamma\chi_b)$				
$1\,^3P_2$	9.8±2.1±2.4	11.4±2.1	5.8±0.7±1.0	6.1±1.4
$1\,^3P_1$	9.1±1.8±2.2	7.8±1.9	6.5±0.7±1.2	5.9±1.4
$1\,^3P_0$	6.4±1.4±1.6		3.6±0.8±0.9	3.5±1.4
$B(\chi_b \to \gamma\Upsilon)$				
$1\,^3P_2$			27±6±6	21±8
$1\,^3P_1$			32+6+7	32±10
$1\,^3P_0$			<6 (90% C.L.)	<10

Table III. Average Measurements of χ_b states.

	$E_\gamma(\Upsilon' \to \gamma\chi_b)$ MeV	$M(\Upsilon') - M(\chi_b)$ MeV	$B(\Upsilon' \to \gamma\chi_b)$ %	$B(\chi_b \to \gamma\Upsilon)$ %
$1\,^3P_2$	109.3±0.5	109.9±0.5	7.0±0.8	24±6
$1\,^3P_1$	130.0±0.6	130.9±0.6	6.8±0.8	32±7
$1\,^3P_0$	161.5±1.3	162.8±1.3	4.0±0.8	<6 (90% C.L.)

exclusive $\gamma\gamma\ell^+\ell^-$ channel from $\Upsilon' \to \gamma\chi_b$, $\chi_b \to \gamma\Upsilon$, $\Upsilon \to \ell^+\ell^-$. The detection of the χ_b states in the inclusive reaction $\Upsilon' \to \gamma\chi_b$ is difficult because of the relatively small branching ratios and the large background of photons from π^0 decays. The exclusive reaction is practically background-free, but has a much lower yield (typically 70 events per χ_b state, compared to ~1000 in the inclusive case).

The best resolution is achieved in the ARGUS and CLEO detectors, where the central drift chambers are used to measure the momenta of e^+e^- pairs from

photons that convert in the material around the beam. Their resolutions for 160 MeV photons are 1.1 and 4 MeV respectively, with efficiencies of 0.9% and 4%. (CLEO inserted extra material to get higher conversion efficiency, at the expense of resolution.) The low efficiency makes only the inclusive channel practical for these detectors.

The results from the individual experiments are shown in Figures 1-4 and and Table II, and the new world averages are given in Table III.

2.2 POTENTIAL MODEL

The potential model consists of a recipe for a potential and calculational means to obtain energies of $q\bar{q}$ states in that potential. The potential is a function of the separation r between the q and $\bar{q}$. Ideas from QCD are used to motivate its form in the two limits $r \to 0$ and $r \to \infty$. In order to calculate quark-spin dependent effects, one needs to decide on a Lorentz structure of the potential: whether it is due effectively to the exchange of vector, scalar, or whatever type particles.

The potential at small r should be due to one-gluon exchange, and thus vector and Coulomb-like[6]: $\frac{-4}{3}\frac{\alpha_s(r)}{r}$. The logarithmic decrease as $r \to 0$ of the QCD coupling constant $\alpha_s(r)$ softens the potential at small r compared to QED[7,8]. QCD corrections up to the order two gluon exchange have been calculated[9,10].

The potential at large r is responsible for keeping the quarks confined. Its Lorentz structure is not easily determined by theory, and is one of the important things we need the data to tell us. Pure scalar confinement[7] has been a popular choice, after pure vector[11] was ruled out by $c\bar{c}$ data. Independent of models, Gromes has shown[12] that the dominant contribution must be vector and/or scalar (unless there are cancellations between leading axial vector and tensor terms.)

Eichten and Feinberg (EF)[13] derived the general form of the spin dependent forces in QCD and found 4 independent terms. As these are not presently calculable, one must make some assumptions to proceed further. EF assumed that confinement is dominated by the longitudinal color-electric field ("electric confinement"), and obtained results different from those of scalar confinement.

In the string or stretched bag picture, the q and $\bar{q}$ are connected by electric flux which, due to the gluon-gluon coupling in QCD, compresses itself into a tube. Its energy is proportional to its length, thus giving a linear contribution kr to the potential. This picture, which is similar to that of EF, was analysed by Buchmüller[14]. Unlike EF, he obtained the same result as for scalar confinement. This discrepancy has been resolved by Gromes[15] in favor of effective scalar, which is also favored in the bag model[16].

Thus the two extremes ($r \to 0, r \to \infty$) are fairly well understood theoretically; unfortunately the experimentally accessible hadrons spend most of their time in the middle. QCD lattice gauge calculations in progress[17] promise to put even this range on a firm footing. Until they are far enough along to provide calculated masses, we rely on potential model as a phenomenological but

useful, successful, and fairly transparent means of understanding heavy quark systems.

There is no one potential model calculation which includes all known effects, but rather numerous calculations, each with its own emphasis. A sampling of the calculations is presented in Table IV. My main goal here is not to compare them all, but to look for a calculation which incorporates the physical ideas mentioned above, and which gives a good description of the data. The calculation of Gupta, Radford and Repko (GRR)[10] uses a linear scalar confining potential, and the Coulomb-like part incorporates the QCD corrections up to the order of two gluon exchange. $\alpha_s(r)$ is used consistently in $V(r)$ and spin dependent terms, and some spin-independent relativistic terms.

2.3 COMPARISON OF χ_b MASSES WITH POTENTIAL MODEL

To compare the χ_b data with the model, it is convenient to use the three quantities defined in Table IV. (For a different approach, see Ref. 24.)

In the absence of spin dependent forces, all 1P states would be degenerate at their center-of-gravity $1\,^3P_{cog}$. The splitting between the S- and P-state center-of-gravities, which would be degenerate for a pure Coulomb force, is determined by the relative strengths of the Coulomb and confining terms in the potential. The GRR calculation[10] obtains M(Υ')-M($1\,^3P_{cog}$)=113 MeV, in good agreement with the measured 123 MeV. Here the Martin potential[19] $V(r) = A + Br^{0.1}$ provides a useful contrast to the more conventional QCD-inspired potentials. It agrees with them well in the middle-r range, but is much softer as $r \to 0$. This leads to a much larger S-P splitting than observed: 164 MeV.

The spin dependent forces split the P states around their center-of-gravity, and are dependent on both the short- and long-range parts of the potential. The relative splitting $\mathbf{r} = \frac{M(^3P_2)-M(^3P_1)}{M(^3P_1)-M(^3P_0)}$ is most convenient for studying the Lorentz structure of the potential. The Coulomb (vector) potential alone would give a relative splitting of $\mathbf{r}$=0.8. Adding a pure vector confining term would increase $\mathbf{r}$ from 0.8 to a maximum of 1.4 as its strength is increased[11], and was ruled out by the χ_c data where $\mathbf{r} = 0.48 \pm 0.01$. A scalar confining term[7] added to the vector Coulomb term can decrease $\mathbf{r}$ enough to fit the χ_c data. The heavier χ_b states have a smaller average radius; thus one would expect them to be less affected by the confining potential and have $0.48 < \mathbf{r} < 0.8$. The CUSB data alone gave a somewhat alarming value[2] of $0.9 \pm 0.1 \pm 0.2$. Now the weighted averages of the χ_b masses yield $\mathbf{r}$=0.66 ± 0.05, which agrees very well with the GRR value of 0.68 for a purely-scalar confining force and rules out purely-vector ($\mathbf{r}$> 0.8).

The absolute splitting M($^3P_2$)-M($^3P_0$) is sensitive to α_s and relativistic corrections, and is thus not well-liked by theorists. Buchmüller[14] obtains values of 38-72 MeV for $\alpha_s(\Upsilon)$=0.28-0.49. GRR use the same α_s in $V(r)$ and the spin dependent terms, and obtain 41 MeV in their semi-relativistic treatment. The relativistic bag model of Baake *et al.*[16] gives 52 MeV, very close to the measured value of 53 ± 2 MeV.

Table IV. χ_b measurements and models.

The experimental $\Gamma(\Upsilon' \to \chi_b)$ was obtained using $\Gamma_{tot}(\Upsilon') = 29.6 \pm 4.7$ keV[18]; the calculations have been adjusted using the measured photon energies. The models are arranged in approximate chronological order. As the models have parameters which need to be fit to the data, this type of comparison is not entirely fair; it is, however, my only possibility. To guide the eye, predictions which come within 10% of the data are underlined.

	mass diff. Υ'-1 $^3P_{cog}$ (MeV)	r = $\frac{^3P_2 - {}^3P_1}{^3P_1 - {}^3P_0}$	mass diff. $^3P_2$-$^3P_0$ (MeV)	sum $\Gamma(\Upsilon' \to \gamma\chi_b)$ (keV)
experiment	122.8±0.4	0.66±0.05	53±2	5±1
Richardson[8] $\alpha_s(r)$ in interpolating form	119			
Martin[19] non-QCD potential	164			
Eichten and Feinberg[13] electric confinement (uncorr.)	96	1.0	50	
with sign of linear contribution to L · S corrected[15]	96	0.80	38	
Baake,Igarashi,Kasperidus[16] relativistic bag model	49	0.73	52	
Gupta Radford and Repko[10] scalar confinement 2-gluon exchange corrections consistent $\alpha_s(r)$, $\Lambda_{\overline{MS}}$=108 MeV				
non-relativistic	113	.68	42	5.7
semi-relativistic	112	.64	41	5.5
Buchmüller,Grunberg,Tye[20] $\alpha_s(r)$ in interpolating form	127			6.0
Buch.[14] scalar confinement $\alpha_s$in spin-dep. = 0.28,0.49		.73, .76	38, 72	
Moxhay and Rosner[21] electric conf. + tensor force relativistic	114	0.42	37	6.9
McClary and Byers[22] 1/r softened by hand linear scalar confinement				
non-relativistic	102			
relativistic corrections	97	0.45	71	5.1
Bander,Silverman,Klima,Maor relativistic[23]				
confinement scalar	132 – 133	.77-.74	62-61	
confinement vector+scalar	134 – 147	.86-.88	69-62	

The strengths of the $\Upsilon' \to \gamma\chi_b$ E1 transitions are dominated by the kinematical E_γ^3 factor. Using the measured E_γ allows one to check the *r*-weighted overlap of the 2S and 1P wave functions. Since the 2S wave function has a node where it changes sign, a cancellation occurs in the overlap integral, which makes it especially sensitive to the detailed shape of the wave functions. Although in the $c\bar{c}$ case only relativistically corrected wave functions gave the right answer[7,22], for $b\bar{b}$ all the calculations are in good agreement with the data.

2.4 χ_b SPINS

Another test of the potential model is the ordering of the χ_b states. Vector forces have the J=0,1,2 states in order of increasing mass; a linear scalar potential that dominated over the Coulomb part would give the opposite ordering[7], and would conflict with the measured spins of the χ_c states. Although the data samples are much smaller for the χ_b states the Crystal Ball collaboration has now succeeded in studying the spins of the $^3P_2$ and $^3P_1$ using the angular correlations in the $\Upsilon' \to \gamma\chi_b$, $\chi_b \to \gamma\Upsilon$, $\Upsilon \to \ell\ell$ decay. They can rule out an inverted spin structure for the χ_b states: the 109 and 130 MeV lines cannot come from spin 0 (C.L.< 0.5%). The combined hypothesis J(109)=1, J(130)=2 is ruled out (C.L.<1.4%, or 2.5 σ from the data), while the expected hypothesis J(109)=2, J(130)=1 agrees with the data to within 0.5 standard deviations. The technique used is difficult to describe succinctly; the interested should read reference 25.

2.5 χ_b HADRONIC WIDTHS

Combining their inclusive and exclusive data, the CUSB and Crystal Ball collaborations can obtain the $B_{\gamma\Upsilon} \equiv B(\chi_b \to \gamma\Upsilon)$, which are given in Table II. These $B_{\gamma\Upsilon}$ are related to the widths of the χ_b states by $B_{\gamma\Upsilon} = \frac{\Gamma_{\gamma\Upsilon}}{\Gamma_{tot}} = \frac{\Gamma_{\gamma\Upsilon}}{\Gamma_{had}+\Gamma_{\gamma\Upsilon}}$. $\Gamma_{\gamma\Upsilon}$ cannot be measured, but can be calculated quite reliably in the potential model since there is no wave function node to cause cancellations[22]. Using $\Gamma_{\gamma\Upsilon}$ from a range of potential models[26,27] one obtains the hadronic widths for the χ_b states given in Table V. (That they are in the 100 keV range, as compared to ~MeV for the χ_c states, is expected due to the heavier quark mass.)

In the QCD picture, the dominant decay of a bound $Q\bar{Q}$ state is $Q\bar{Q}$ annihilation into the smallest allowed number of gluons, because that gives the smallest suppression due the factor of α_s which appears at each vertex. One calculates the decay into on-shell massless gluons, and assumes that the process of turning gluons into hadrons does not affect the rate. (This is the same type assumption made in calculating $e^+e^- \to$ hadrons.) One also assumes factorization; i.e. that the annihilation of the $Q\bar{Q}$, which occurs at small separation ($\sim 1/m_Q$), is not affected by their confinement within a ~1 fm hadron. The annihilation is calculated in the zero binding limit, where the quarks are at rest. The wave function of the confined quarks enters only as the probability

Table V. χ_b and χ_c State Hadronic Widths

The $|\Psi'(0)|^2$ and $B_{\gamma\Upsilon}$ are calculated in potential models in references 10, 20, 21, 22, 26, 35; the error indicates the variation among them. The QCD values are from formulae in references 28, 30, 31; the errors quoted include only the errors on α_s and $|\Psi'(0)|^2$. I used for $b\bar{b}$ $|\Psi'(0)|^2 = 1.39\pm0.05$ GeV^5 and $\alpha_s(0.48M_\Upsilon) = 0.165\pm0.005$; and for $c\bar{c}$ $|\Psi'(0)|^2 = 0.08\pm0.03$ GeV^5 and $\alpha_s(0.44M_\psi) = 0.22\pm0.01$. α_s was obtained from $B_{\mu\mu}$ as in ref. 33. The Γ_{had} were calculated using the χ_{cog} mass; using the $^3P_0$ mass instead would increase the $^3P_0$ width by <1% for χ_b and ~13% for χ_c.

χ_b	(Γ's in keV)	$^3P_2$	$^3P_1$	$^3P_0$	$^3P_0/^3P_2$
measured	$B_{\gamma\Upsilon}$	.24±.06	.32±.07	<.06	
calculated	$\Gamma_{\gamma\Upsilon}$	39±6	33±5	27±5	
derived $\Gamma_{had}=$	$\Gamma_{\gamma\Upsilon}(\frac{1}{B_{\gamma\Upsilon}}-1)$	123±45	70±23	>345	>2
0^{th} order QCD	Γ_{had}	101±7	~ 40	378±26	3.75
1^{st} order QCD	Γ_{had}				5.6
χ_c	(Γ's in MeV)	$^3P_2$	$^3P_1$	$^3P_0$	$^3P_0/^3P_2$
measured[18]	$B_{\gamma\psi}$	.16±.02	.28±.03	.008±.003	
calculated	$\Gamma_{\gamma\psi}$	.48±.13	.36±.10	0.18±0.05	
derived $\Gamma_{had}=$	$\Gamma_{\gamma\psi}(\frac{1}{B_{\gamma\psi}}-1)$	2.5±0.8	0.9±0.3	22±10	9±5
Total width measurements					
R704 $p\bar{p}$[36]	Γ_{tot}	3^{+2}_{-1}	<1.3		
CB incl. γ[37,38]	Γ_{tot}	1-5	<4	13-20	3-24
CB excl. γ[39]	Γ_{tot}	4±1	<2.6		
CB $\pi^0\pi^0$[40]	Γ_{tot}			9±2	
average	Γ_{tot}	3.6±0.8	<1.3	11±2	
measured $\Gamma_{had}=$	$\Gamma_{tot}(1-B_{\gamma\psi})$	3.0±0.7	<1.0	11±2	4±1
0^{th} order QCD	Γ_{had}	.64±.25	~0.2	2.4±0.9	3.75
1^{st} order QCD	Γ_{had}				6.9
measured[40]	$B^*_{\gamma\gamma}$	10±5		4.5±3.0	0.5±0.4
measured $\Gamma^*_{\gamma\gamma}/\Gamma_{had}=$	$B^*_{\gamma\gamma}/(1-B_{\gamma\psi})$	12±6		4.5±3.0	0.4±0.3
0^{th} order QCD	$\Gamma^*_{\gamma\gamma}/\Gamma_{had}$	10		10	1.0
1^{st} order QCD	$\Gamma^*_{\gamma\gamma}/\Gamma_{had}$				0.7

* The $B_{\gamma\gamma}$ and $\Gamma_{\gamma\gamma}$ are in units of 10^{-4}.

of both quarks being at the same point: $|\Psi(0)|^2$ for S states, and $|\Psi'(0)|^2$ for P states (where $|\Psi(0)|^2=0$).

The $^3P_2$ and $^3P_0$ states can decay into two gluons. The rates have been

calculated to 0^{th} order in QCD by Barbieri *et al.*[28]:

$$\Gamma^0_{had}(^3P_2) = \frac{128}{5}\frac{\alpha_s^2}{M_\chi^4}|\Psi'(0)|^2, \quad \Gamma^0_{had}(^3P_0) = \frac{15}{4}\,\Gamma^0_{had}(^3P_2).$$

Since a spin one particle is forbidden to decay into 2 massless vector particles[29], the $^3P_1$decays into ggg or $q\bar{q}g$. (The ggg decay is *not* forbidden by C-parity. Since a gluon is not necessarily its own antiparticle, it needn't be in an eigenstate of C-parity. The color state of a system of three gluons can be arranged to to give C=+ or C=-.) Barbieri *et al.*[30] have shown that the $q\bar{q}$ decay dominates, since it has a logarithmic divergence in the zero binding limit ($2m_b = M_\chi$). Since this last equality is approximately satisfied, and in fact all these calculations are based on the 'zero binding approximation', this is a very unhealthy situation. The most that one can say for sure is that, since the ggg channel has no such divergence, the $q\bar{q}g$ will dominate. The formula is

$$\Gamma^0_{had}(^3P_1) = \frac{n_f}{3}\frac{128}{3\pi}\frac{\alpha_s^3}{M_\chi^4}|\Psi'(0)|^2\ln\left(\frac{4m_b^2}{4m_b^2 - M_\chi^2}\right)$$

where n_f is the number of light flavors (4 for χ_b decays). To get an idea of the expected width, I can use the fact that the Υ'' is bound, so that $m_b > M(\Upsilon'')/2$, and $\Gamma_{had}(^3P_1)<29$ MeV. Using the approximations mentioned in reference 30 and 31 that $\ln\left(\frac{4m_b^2}{4m_b^2-M_\chi^2}\right) \approx -2\ln(\alpha_s)$ or $\approx \ln(m_b R_c)$ where $R_c \sim (0.4\text{GeV})^{-1}$ is the confinement radius, I get $\Gamma_{had}(^3P_1)$=42 MeV or 30 MeV. The measured 70 ± 25 is in this general area.

The next-order QCD calculations[31] are not straightforward:

- The logarithm mentioned above also multiplies the QCD correction to the $^3P_2$ and $^3P_0$ widths.
- A term inversely proportional to the relative quark velocity v appears. This becomes divergent in the zero-binding ($2m_Q = M_\chi$) limit. In a bound-state calculation this is naturally absorbed into the wavefunction. However it is well known that other terms of unknown magnitude might also be absorbed[32]. To avoid this unknown constant, we can consider only ratios, where the dependence on the wave function divides out.
- We use the scale $Q=0.48\,M_\Upsilon$ chosen by Mackenzie and Lepage[33] to make the 1^{st} order QCD corrections for the hadronic width of the Υ vanish, and the resulting $\alpha_s(Q=0.48M_\Upsilon)=0.165$. However, in a later paper[34], Brodsky, Mackenzie and Lepage decided upon a different scheme for optimizing the choice of scale; their prescription gives very large corrections for Υ[34] and χ_b[32] widths. Actually there is no fool-proof way of choosing the Q or the renormalization scheme. The real solution lies in calculating to enough orders so that these no longer matter, but that is very difficult.
- Even with the choice $\alpha_s(Q=0.48M_\Upsilon)=0.165$, the correction to the ratio of $^3P_2$ and $^3P_0$widths is large enough to make one want the next next order calculation.

▷ The corrections for the $^3P_1$ have not been done.

Given this long list of problems, the agreement evident in Table V is surprising. The $b\bar{b}$ $^3P_2$ hadronic width agrees very well with the 0^{th} order calculation; the lower limit on the $^3P_0$ is just below the expected value.

In the $c\bar{c}$ case, the hadronic widths can not only be derived from the $B_{\gamma\psi}$'s and the calculated $\Gamma_{\gamma\psi}$'s as for $b\bar{b}$, but can also be extracted from direct χ_c total width measurements. The two methods are compared in Table V, and agree well. The later gives the more precise result for the $^3P_0$. Both the $^3P_2$ and $^3P_0$ have hadronic widths which are about a factor of 4 higher than expected from 0^{th} order QCD using the α_s which fits the J/ψ width. This disagreement is thought to be due to relativistic corrections to the wave function[26].

The wave function divides out of the following ratios:

$$\frac{\Gamma^1_{had}(^3P_0)}{\Gamma^1_{had}(^3P_2)} = \frac{15}{4}(1 + 9.5\frac{\alpha_s}{\pi}) \qquad \text{for } b\bar{b}$$

$$= \frac{15}{4}(1 + 12\ \frac{\alpha_s}{\pi}) \qquad \text{for } c\bar{c}$$

$$\frac{\Gamma^0_{\gamma\gamma}(^3P_0)}{\Gamma^0_{had}(^3P_0)} = \frac{\Gamma^0_{\gamma\gamma}(^3P_2)}{\Gamma^0_{had}(^3P_2)} = \frac{9}{2}e_Q^4(\frac{\alpha}{\alpha_s})^2$$

$$\frac{\Gamma^1_{\gamma\gamma}(^3P_0)}{\Gamma^1_{\gamma\gamma}(^3P_2)}\frac{15}{4} = (1 + 5.5\frac{\alpha_s}{\pi}) \qquad \text{for } c\bar{c}$$

$$\frac{\Gamma^1_{\gamma\gamma}(^3P_2)/\Gamma^1_{had}(^3P_2)}{\Gamma^1_{\gamma\gamma}(^3P_0)/\Gamma^1_{had}(^3P_0)} = 1 + 4.0\frac{\alpha_s}{\pi} \qquad \text{for } b\bar{b}$$

$$= 1 + 6.5\frac{\alpha_s}{\pi} \qquad \text{for } c\bar{c}$$

In both the $b\bar{b}$ and $c\bar{c}$ cases, the ratio $\Gamma_{had}(^3P_0)/\Gamma_{had}(^3P_2)$ is in good agreement with the 0^{th}order QCD prediction and, curiously, in less good agreement with the 1^{st} order prediction. The branching ratio of $\chi_c \rightarrow \gamma\gamma$ has been measured, although with large errors, and agrees well with the prediction.

The experimental error might be improved in many cases, especially the total widths of the χ_c (see following section); the prospects for improving the large theoretical uncertainties are less good. However, perhaps the data is trying to tell us that the $Q \sim \frac{1}{2}M_\Upsilon$ scale is the right one.

2.6 P STATES OF $c\bar{c}$

The last ISR experiment R704 pioneered a new technique of observing $c\bar{c}$ P states[36]. They produce them directly in $p\bar{p}$ annihilation, scanning the beam energy over the expected mass region. Their scans of the χ_c $^3P_2$ and $^3P_1$, shown in Figure 5, are quite impressive. The χ_c states are identified by their decay to $\gamma\psi$, $\psi \rightarrow e^+e^-$. The fitted masses are 3511.4 ± 0.6 and 3556.8 ± 0.6 MeV. The ISR beam gives them a mass resolution of ~0.3 MeV, allowing them to

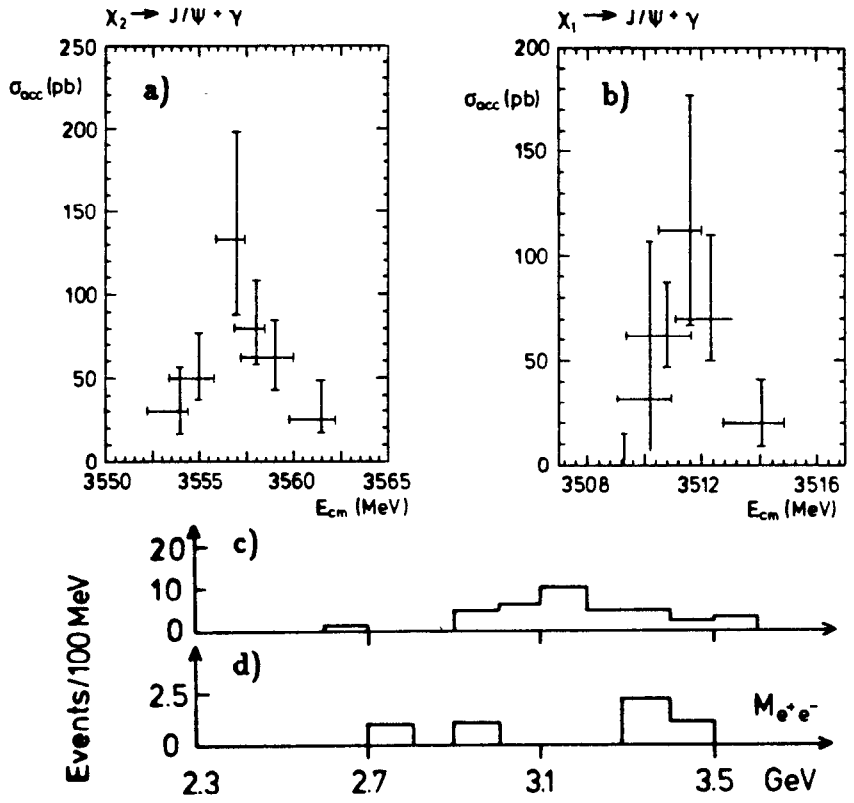

Figure 5. R704 P states. (**a**) $p\bar{p} \rightarrow \gamma\psi$ cross section in $^3P_2$ region. The plot contains 56 candidates, with an estimated background < 2. (**b**) $^3P_1$ region, with 32 candidates, < 2 background. (**c**) e^+e^- mass for $^3P_1$ candidates. (**d**) for $^1P_1$ candidates.

measure the total widths of these states, which were discussed in the previous section and Table V. These results were obtained with only a few weeks running time. More data would certainly improve the width measurements.

We still have no definite evidence for a $^1P_1$ state. Most calculations put this state within a few MeV of the $^3P_{c\bar{c}g}$, and a deviation from this would cause an uproar. The $b\bar{b}$ state might be see-able in the decay $\Upsilon'' \rightarrow \pi\pi\ ^1P_1$, but so far no experiment has enough resolution times Υ'' data. In the $c\bar{c}$ case, kinematics and quantum numbers conspire to give us no reasonable way of producing this state at e^+e^- machines.

The R704 scan for the $^1P_1$ suffered from lack of time. They could not get as much data, especially off-resonance, as one would like for this important discovery. Since the $\gamma\psi$ decay is forbidden, they used cuts designed to accept decays to $\pi^0\psi$ or $\pi^0\pi^0\psi$. They required identified e^+e^-, and no other charged tracks. Their acceptance is good for e^+e^- masses above 2.3 GeV. With 710 nb^{-1} of data at the expected $^1P_1$ position (3524-3527 MeV) they obtained 5

events with e^+e^- masses in the J/ψ region, and none with e^+e^- masses between 2.3 and 2.6 GeV (Figure 5d). The main background is expected to be non-resonant $\pi^0\psi$ production. To study this, they collected 300 nb^{-1} to either side of the expected mass (3519-3524 and 3527-3531) and found no candidates. Using as additional "background" their $^3P_1$ data, removing the events identified as $\gamma\psi$ and applying their $^1P_1$ selection criteria, they also find no candidates. They derive an upper limit of 2 background events (90% C.L.) among their 5 candidates at 3524-3527 MeV. As the ISR is now permanently shutdown, they can't get any more data there. LEAR is at too low an energy, but the Fermilab $\bar{p}$ accumulator may be a suitable place to continue this promising line of experimentation.

2.7 PERSPECTIVES ON HEAVY QUARKS

The non-relativistic potential model for heavy quarks is now slighty over 10 years old. It was born[6] approximately simultaneously with the J/ψ and ψ' particles, and grew up with the $c\bar{c}$ family as it increased to include χ_c and η_c states. Investigations soon began on how to calculate the spin-dependence[41,11,7,42]. The situation was confused by the observation[43] of the now-deceased $\chi(3455)$ and the X(2800), early candidates for the η_c' and η_c. By 1979 there was enough high-precision data[44] available to fix the χ_c and η_c at their present positions, where they reside in happy agreement with model calculations using a Coulomb plus scalar confining potential. The $\psi' \rightarrow \gamma\chi_c$ transition rates were a factor-of-two problem, which was solved by calculating[7,22] the relativistic corrections to the $c\bar{c}$ wave functions.

The discovery of the Υ family in 1977 was welcomed as an independent test of the potential model, especially of its flavor-independence, and in a regime where relativistic corrections are smaller. First measurements[2] of the χ_b states gave results which did not agree too well with the scalar confinement form which worked so well for the χ_c states. Nevertheless, recent clarifying work[15] has brought the followers of bags, strings, and Wilson loops into agreement that the the confining force should be scalar. New measurements[3,5] of the χ_b states, presented at this conference, now bring them into good agreement with this expectation.

One remaining problem in the $c\bar{c}$ system is the hadronic widths of the χ_c states, which are much larger than predicted. That this is due to relativistic effects distorting the wave functions has been speculated, but not demonstrated. The less relativistic χ_b states have widths in good agreement with expectations. However these calculations, like those of the Υ width, are subject to large theoretical uncertainties in the QCD corrections. Since we are more interested in QCD **theory** than in potential **models**, it would be nice if these calculations could be straightened out. I am told this would be very difficult. The solution to the theory-model dilemma may be on the way from another direction, which is also very difficult: that of lattice gauge calculations, which are gradually achieving greater reliability.

The Υ family seems to be a good compromise between $c\bar{c}$, which is somewhat too light for reliable calculations, and the top system which, wherever

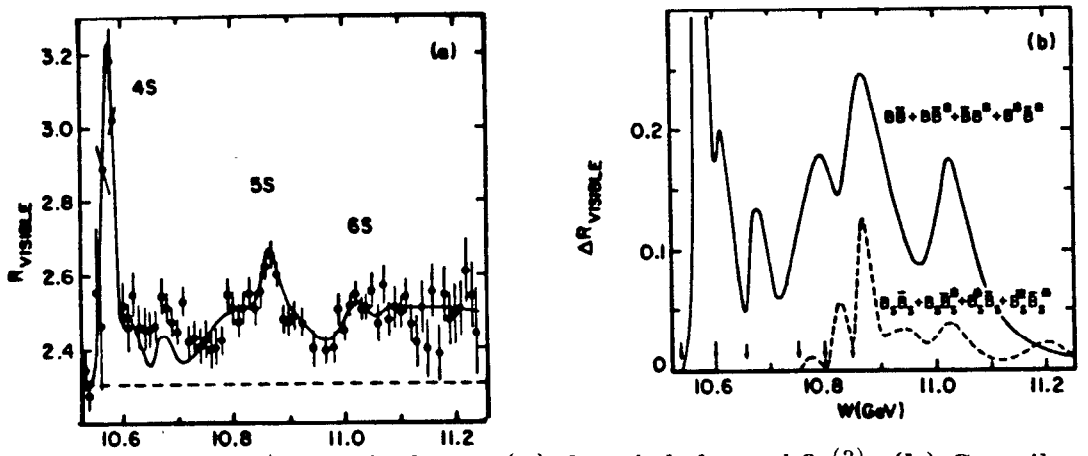

Figure 6. CUSB $e^+e^- \rightarrow$ hadrons. **(a)** Coupled channel fit[2]. **(b)** Contributions to (a) from B, B^*, B_s, B_s^*.

it is, will be even more difficult experimentally. Recent work has helped considerably to clarify both the experimental and theoretical view of heavy quark systems, and I hope this trend will continue.

3. OTHER HEAVY STATES

3.1 HIGHER MASS UPSILON STATES

CLEO[45] and CUSB[46] have scanned the region above the $\Upsilon(4S)$ and found evidence for higher mass Υ's. CUSB has performed a coupled channel fit to their data (Figure 6), including significant effects from $\Upsilon(5S)$, $\Upsilon(6S)$, and the various $B_{(s)}^{(*)}\bar{B}_{(s)}^{(*)}$ thresholds. With so much activity expected from "normal" sources in this region, it will unfortunately be very difficult to obtain information on predicted $b\bar{b}g$ states[47].

3.2 B^*, F^*, D^{**}, AND MAYBE Ω^*

Last year CUSB obtained evidence for a B^* meson 50 MeV above the B[48]. It was observed in the inclusive photon spectrum of hadronic events taken at center-of-mass energies above 10.6 GeV. In a second analysis, they use the semi-leptonic decay of the B to increase the signal to background ratio by 4 (at an expense of a factor of 10 in statistics) by requiring a > 1 GeV electron. The resulting photon spectra[2] are shown in Figure 7. The signal has a significance of 7σ in the total inclusive sample and 4.4σ in the electron-tagged sample. The number of B^*'s per non-continuum event are 1.5 ± 0.3 and 1.5 ± 0.5 in the two samples, and the photon energy corresponds to a $B^* - B$ mass difference of $52.5\pm2\pm4$ MeV. Since the B's are not identified in this analysis, it is not known if this mass difference applies to charged or neutral B's, or, most likely, to both.

ARGUS has available for this conference evidence for a D^{**} meson at 2421 ± 7 MeV, shown in Figure 8. Since it is seen in B-jets, it is discussed more fully in David Saxon's review of jet fragmentation at this conference.

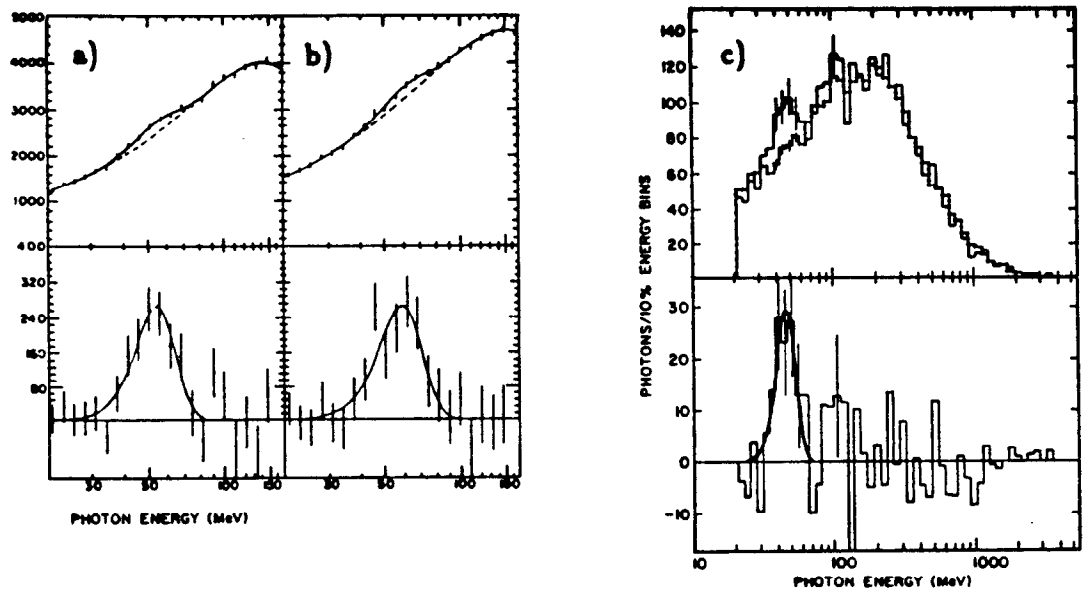

Figure 7. CUSB B^* signal[2] (a) in inclusive photon spectra for $10.77 < E_{cm} < 10.89$ GeV (4.7σ, $51\pm2\pm5$ MeV). (b) for $10.985 < E_{cm} < 11.255$ GeV (3.9σ, $53\pm2\pm5$ MeV). (c) in lepton-tagged events.

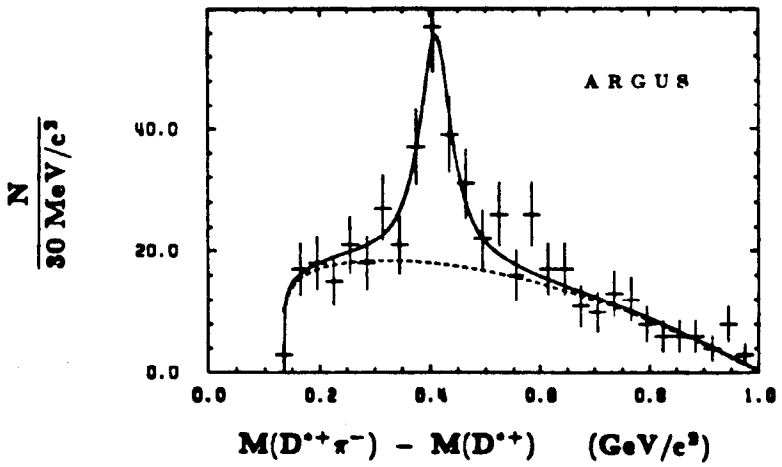

Figure 8. ARGUS D^{**} signal.

The LASS collaboration has reported[55] at this conference a 4σ signal in $K\Xi^{*0}$ at 2.26 GeV. This is one of the expected decay channels for an Ω^*, and is in the expected mass range. The collaboration has only analysed the first half of their huge data sample (10^8 events, $5nb^{-1}$). As the second half should be ready within a few months, it would be wise to wait until then before getting excited.

These $Q\bar{q}$ mesons provide a new spectroscopy where the potential model can be tested. Rather than go into that here, I take a very phenomonological view in the following.

Table VI. $Q\bar{q}$ Meson Masses

Meson	Mass in MeV	Decay	Experiment
B^*	B + 52.5 ± 2 ± 4	Bγ	CUSB[48]
B^0	5274 ± 2 ± 2	$D^{*-}\pi^+$	CLEO[49]
B^+	5271 ± 2 ± 2	$D^{*-}\pi^+\pi^-$	CLEO[49]
F^*	F + 144 ± 9 ± 7	Fγ	ARGUS[50]
	F + 140 ± 8 ± 10		TPC[51]
	2113 ± 9		average
F	1971 ± 2	$\phi\pi$,$\phi 3\pi$,KKπ	average[52]
D^{*-}			ARGUS[53]
D^{*+}	2010.1 ± 0.7		average[54]
D^{*0}	2007.2 ± 2.1		average[54]
D^+	1869.4 ± 0.6		average[54]
D^0	1864.7 ± 0.6		average[54]

Combining all the vector-pseudoscalar mass differences for mesons containing a light quark, one finds an amazingly regular pattern for the hyperfine splittings:

$$\rho^2 - \pi^2 = .57 \text{ MeV}^2$$
$$K^{*2} - K^2 = .56$$
$$D^{*2} - D^2 = .55$$
$$F^{*2} - F^2 = .58 \pm .04$$
$$B^{*2} - B^2 = .55 \pm .04$$

The pattern is broken for cases where there is SU(3) octet-singlet mixing:

$$(\omega, \phi)^2_{ave} - (\eta, \eta')^2_{ave} = .25$$

or where both quarks are heavy:

$$\psi^2 - \eta_c^2 = .70 \pm .04$$
$$(\psi')^2 - (\eta_c')^2 = .67 \pm .04$$

There are explanations for this[56]. Nevertheless I am still amazed it actually works from 5 GeV all the way down to the π mass. Certainly the light quark systems will prove to be much more difficult in the rest of my talk.

3.3 SEARCH FOR HEAVY PARTICLES IN RADIATIVE Υ DECAYS

Last summer the Crystal Ball reported[57] evidence for a narrow resonance at 8.3 GeV, which they called the ς. It appeared as a 4σ peak in the inclusive photon spectrum $\Upsilon \to \gamma$+hadrons, and again with 3σ in an independent sample selected for low multiplicity. The CESR and DORIS experiments have now collected 2-3 times the original data samples, and no signal is seen[58]. The upper limits for $\Upsilon \to \gamma\varsigma$ are near 0.1%, substantially below the original Crystal Ball value of ~0.5%.

The same Υ data samples can be used to look for $\Upsilon \to \gamma$+Higgs. The ARGUS and CUSB data cover the largest mass range. Their results are compared in Figure 9 to the Wilzcek[59] Standard Model calculation of $\Upsilon \to \gamma$+Higgs. This

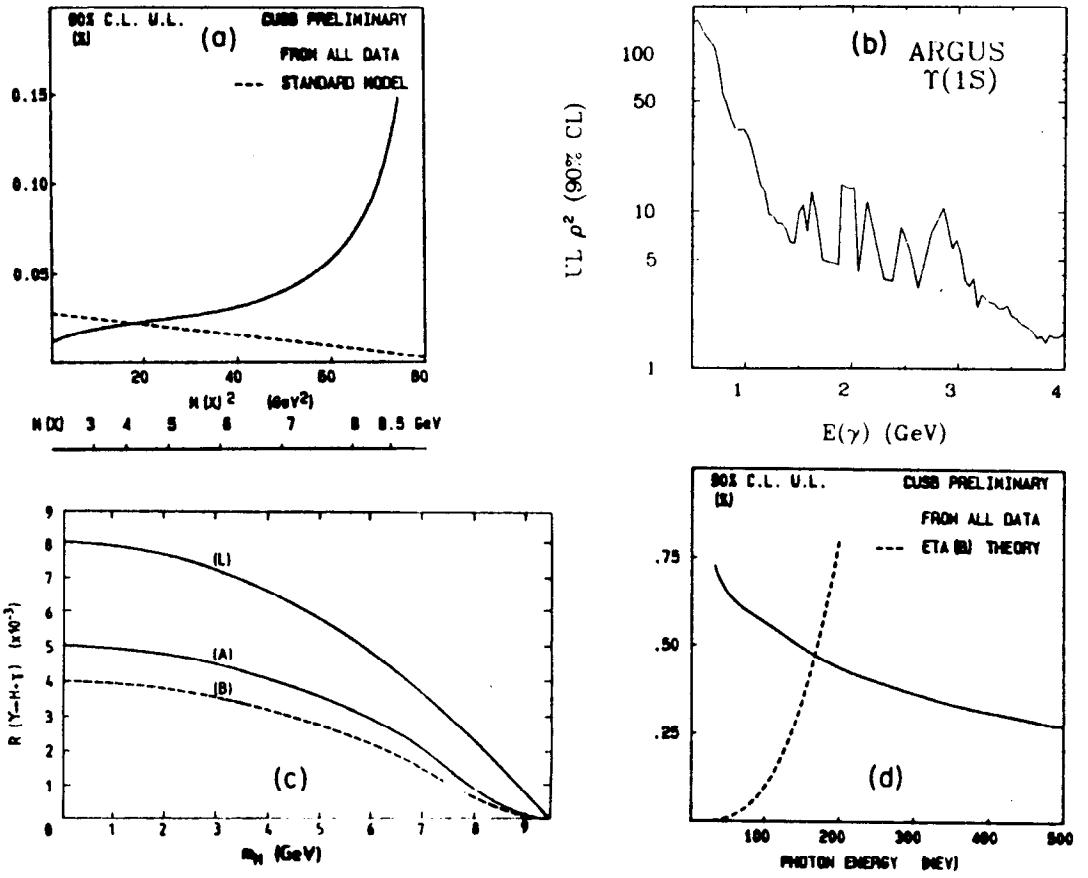

Figure 9. (a) CUSB preliminary upper limit on BR($\Upsilon \rightarrow \gamma$ + narrow state). The lower line is the Wilzcek BR($\Upsilon \rightarrow \gamma$ + Higgs). (b) ARGUS upper limit on ρ^2 = BR($\Upsilon \rightarrow \gamma$ + narrow state) / Wilzcek BR($\Upsilon \rightarrow \gamma$ + Higgs). (c) BR($\Upsilon \rightarrow \gamma$ + Higgs) / BR($\Upsilon \rightarrow \mu\mu$) of Wilzcek (L) and (A)-(B) after QCD and mixing corrections[60]. (d) CUSB upper limit for $\Upsilon \rightarrow \gamma$ + narrow state compared to the expected $\Upsilon \rightarrow \gamma\eta_b$. The η_b is expected to be 20-100 MeV below the Υ.

calculation does not include QCD corrections and mixing effects[60] which reduce the rate by about a factor of 2. Thus the available data is not yet sensitive enough to rule out Standard Higgs production in Υ decays. The limits are interesting in models with two Higgs doublets, where BR($\Upsilon \rightarrow \gamma$H) can be larger than in the standard one-doublet model[61].

3.4 THE $\xi(2.2)$ IN RADIATIVE J/ψ DECAYS

Two years ago the Mark III collaboration reported[62] a $\sim 7\sigma$ signal in radiative J/ψ decays for a heavy narrow resonance decaying into $K\bar{K}$, which they named the ξ. The reported mass and width were $2220 \pm 15 \pm 20$ MeV and $30 \pm 15 \pm 20$ MeV respectively, with a branching ratio $\psi \rightarrow \gamma\xi$, $\xi \rightarrow K^+K^-$ of $(8 \pm 2 \pm 2) \times 10^{-5}$. Subsequent re-evaluation of that data[63,64] yielded a statistical significance of 4.6σ and the revised parameters M = $2218 \pm 3 \pm 10$ MeV,

Γ<40 MeV (95% C.L.), and branching ratio $(3.8\pm1.3\pm0.9)\times10^{-5}$.

Their observation of this signal relied heavily on making maximum use of the advantages of their detector (summarized in Table VII). To eliminate $\pi^+\pi^-$ background they required that each "K" be within 2.5σ of the expected TOF for a kaon, and be closer to the expected TOF of a kaon than to that of a pion. A kinematic fit to the γK^+K^- state, imposing energy and momentum conservation, improves the mass resolution for the ξ from ~30 to ~10 MeV, and also removes some backgrounds. The resulting efficiency is about 30% in the ξ region. The main background there comes from $K^+K^-\pi^0$ events (dominantly KK^*) with a missing γ.

The Mark III collaboration has three sets of J/ψ data. In the 1982 sample of 0.8 million J/ψ's, the ξ appears 40 MeV higher in mass than in the 1983 sample (1.8 million J/ψ's)[63]. This shift is outside the systematic error of 10 MeV and no explanation has been found. However the 1982 data *was* the first physics data taken with the new detector, and the 1983 sample *does* have higher statistics. The 1985 sample of 3.3 million J/ψ's was not ready to present at this conference, due to problems with the TOF and drift chamber resolutions. **Results were presented[65] at the later SLAC and Kyoto conferences, confirming the existence of the $\xi(2.2)$ in the new Mark III data.**

The DM2 collaboration[66] has analysed 8.7 million ψ decays. They see no evidence for the $\xi(2.2)$, and place upper limits $BR(\psi\rightarrow\gamma\xi,\ \xi\rightarrow K^+K^-) < 1.2\times10^{-5}$ (95% C.L.) assuming a ξ width narrow compared to their mass resolution of 12 MeV. They achieve this mass resolution via a kinematic fit, as does Mark III. DM2 also use the fit to remove pion backgrounds by requiring that each event fit the γK^+K^- hypothesis but not the $\gamma\pi^+\pi^-$ one. This cut against $\pi^+\pi^-$ reduces their efficiency a higher masses, and is a cut not made by Mark III. Another difference is in the TOF requirement; DM2 requires only that one of the two charged tracks be compatible with TOF expected of a kaon. One would expect this to give them more background above 2 GeV than Mark III has. This is not evident in Figure 10. However it is not possible to compare backgrounds without knowing the efficiencies. That of DM2 drops a factor of 2 between 2 and 2.5 GeV. In any case, a properly computed upper limit takes all this into account.

DM2 has also analysed $\psi\rightarrow\gamma K_SK_S$, shown in Figure 10c. Here their KK mass resolution is 11 MeV. An isoscalar ξ would have equal branching ratios to $K^+\bar{K^-}$ and $K^0\bar{K}^0$. The peak evident in the 2.2 GeV region is one bin (30 MeV) too low to be the ξ. Using that bin anyway to calculate their upper limit, and correcting for $K_SK_S/K^0\bar{K}^0 = 1/2$, DM2 obtains $BR(\psi\rightarrow\gamma\xi,\ \xi\rightarrow K^0\bar{K}^0) < 2.0\times10^{-5}$ (95% C.L., assuming zero width).

It is unlikely, but not totally inconceivable, that 3.8-1.3-0.9 <1.2. If both experiments are right, something has to give. One interesting variable is the width of the ξ which is assumed to be zero in the DM2 limit. Given the interest in this state (possible explanations include Higgs with enhanced hadronic decay, high-spin $s\bar{s}$ state, glueball decaying preferably to $s\bar{s}$), one hopes that a definite resolution to the experimental conflict can be found soon.

Table VII. Mark III and DM2 Detectors.

	Mark III	DM2
charged tracking		
momentum resol. at 1 GeV	2.1%	3.5%
for solid angle	85%	87%
shower counters		
energy resol. at 1 GeV	18%	35%
position resol. in ϕ	7 mrad	10 mrad
position resol. in θ	20 mrad	7 mrad
solid angle	93%	70%
Time-Of-Flight system		
time resolution	190 ps	540 ps
π/K separation	2σ at 1.0 GeV	3σ at 0.45 GeV
solid angle	80 %	

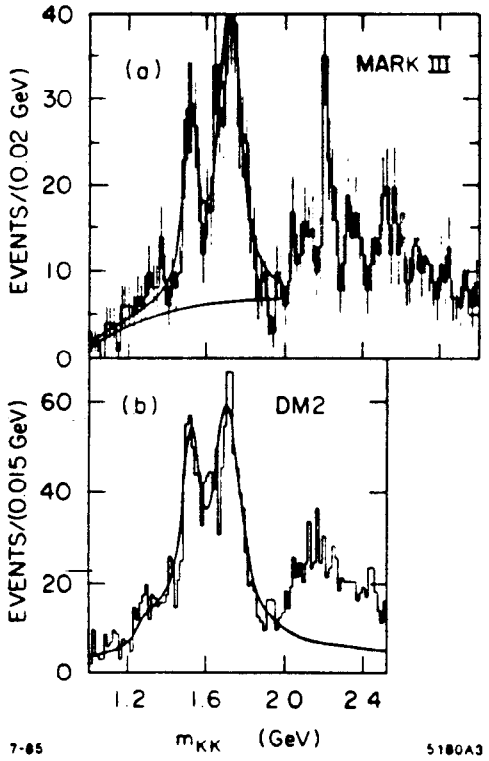

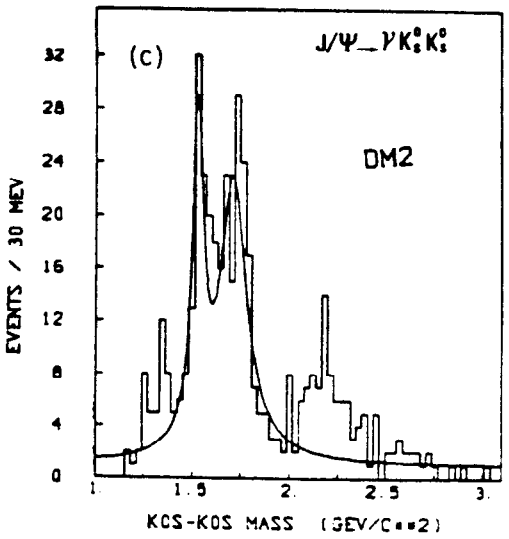

Figure 10. $\psi \to \gamma KK$. (a) Mark III K^+K^- mass spectrum[64]. (b) DM2 K^+K^- spectrum. (c) DM2 K_SK_S spectrum[66].

4. THE E(1420) AND THE ι(1460)

The E(1420) and the ι(1460) are both $K\bar{K}\pi$ resonances but, as their names indicate, have been regarded as different resonances. This is partly on the basis of the slightly higher mass and width of the ι:

$$M(\iota) = 1458 \pm 6, \quad \Gamma(\iota) = 97 \pm 13 \text{ MeV}$$
$$M(E) = 1418 \pm 4, \quad \Gamma(E) = 52 \pm 5 \text{ MeV}.$$

I don't find this evidence overwhelming, since the mass difference is within the ι width. There are other particles such as the ρ which appear with different masses in different reactions.

The main differentiation comes from the evidence of their spins and decays. The experiments which observe the ι in radiative J/ψ decay agree on assigning it $J^P=0^-$, with indications for $\delta\pi$ substructure in the $K\bar{K}\pi$ decay. The E is more controversial. It was first assigned $J^P=0^-$ by a $p\bar{p}$ experiment[67]. Later π^-p experiments[68] gave it $J^P=1^+$, including a recent high statistics π^+p experiment[69]. Now an even higher statistics π^-p experiment[70,71] has measured $J^P(E) = 0^-$. The decay channel also changes from $K^*\bar{K}$ (and its charge conjugate, which will always be implied in the following) to $\delta\pi$.

If this latest result is the correct one, it is possible that the E and ι are the same particle. In the following I will review the state of our knowledge of these resonances. Section 4.1 deals with the $K\bar{K}\pi$ channel, which provides the strongest evidence for the E and the ι, and is used for the spin determinations. Section 4.2 covers the confusing $\eta\pi\pi$ channel, and section 4.3 the $\gamma\rho$, $\rho\rho$, and $\omega\omega$ enhancements. Finally in 4.4 I try to draw some conclusions on where we stand with the E and ι.

4.1.1 $\psi \to \gamma\,\iota$, $\iota \to K\bar{K}\pi$

A $K_S K^\pm\pi^\mp$ resonance was first seen in radiative J/ψ decays at ~1440 MeV by the Mark II[72]. Speculation began at once that this state is a glueball, since it is the largest radiative J/ψ decay (except for $\psi\to\gamma\eta_c$, which doesn't require $c\bar{c}$ annihilation). The $K\bar{K}$ are produced preferentially with low mass, as though the decay were $\iota\to\delta\pi$, $\delta\to K\bar{K}$. The Crystal Ball[73] confirmed this, and performed a spin parity analysis in 100 MeV bins of the $K^+K^-\pi^0$ final state using the isobar model, where all decays are assumed to be via a two body intermediate state, i.e. $\delta\pi$ or K^*K. They included $J^P = 0^-$ and 1^+, and $K\bar{K}\pi$ phase space. The peak occurs in the $\delta\pi(0^-)$ channel, and the K^*K contribution is small and flat.

The DM2[66] and Mark III[74] collaborations have now measured $\psi\to\gamma\iota$, $\iota\to K\bar{K}\pi$ with higher statistics. Whereas the earlier mass and width measurements were consistent with those of the established E meson, the new ones are higher (Table VIII). This might be because they have higher statistics and are simply better. It might also be that the earlier measurements were biased by the low mass $K\bar{K}$ cuts used. Mark III[74] observe a 14±7 MeV downward shift

Table VIII. Properties of ι in Radiative J/ψ Decay.

Branching ratios $\psi \to \gamma\iota$ are for a spin 0 ι, which gives a $1+\cos^2\theta$ distribution. The ι decay ratios assume the ι has I=0 and thus $(\delta\pi)^0 = \frac{1}{3}\delta^0\pi^0 + \frac{2}{3}\delta^\pm\pi^\mp$. and $(K\bar{K}\pi)^0 = \frac{1}{3}K_SK^\pm\pi^\mp + \frac{1}{3}K_LK^\pm\pi^\mp + \frac{1}{6}K^+K^-\pi^0 + \frac{1}{6}K^0\bar{K}^0\pi^0$. C = + gives $K^0\bar{K}^0\pi^0 = \frac{1}{2}K_SK_S\pi^0 + \frac{1}{2}K_LK_L\pi^0$. Masses and widths are in MeV. Upper limits are 90% confidence level.

	Mark II	Crystal Ball	Mark III	DM2
References	72	73, 75, 76	74,77	66
no. of $\iota \to K_SK^\pm\pi^\mp$ events	~85		340±18	798±36
no. of $\iota \to K^+K^-\pi^0$ events		174±30	402±20	374±46
Mass in $K\bar{K}\pi$	1440^{+10}_{-15}	1440^{+20}_{-15}	1456±5±6	1460±3±8
Width	50^{+30}_{-20}	55^{+20}_{-30}	95±10±15	100±12±15
for M(KK)	<1050	<1125	<1320	<1350
J^{PC}		0^{-+} for isobar anal.	0^{-+}	consistent with 0^{-+}
$B(\psi \to \gamma\iota,\ \iota \to K\bar{K}\pi) \times 10^3$	4.3±1.7	4.0±0.7±1.0	5.0±0.3±0.8	4.1±0.6±0.9
$B(\psi \to \gamma D,\ D \to K\bar{K}\pi) \times 10^3$	<0.7			
$B(\psi \to \gamma\eta') \times 10^3$		4.1±0.3±0.6	4.7±0.2±0.7	4.7±0.5±1.0
$B(\psi \to \gamma\eta) \times 10^3$		0.9±0.1	0.9±0.2±0.2	0.8±0.1±0.2
$\iota \to K^*K/(K^*K + \delta\pi, \delta \to K\bar{K})$		<0.25		
$\iota \to K^*K/K\bar{K}\pi$			<0.35	
for M($K\bar{K}\pi$)		1400-1500	1200-1600	
$\iota \to \eta\pi\pi / K\bar{K}\pi$	<1.1	<0.5	<0.26	
$\iota \to (\delta\pi, \delta \to \eta\pi) / K\bar{K}\pi$			<0.14	

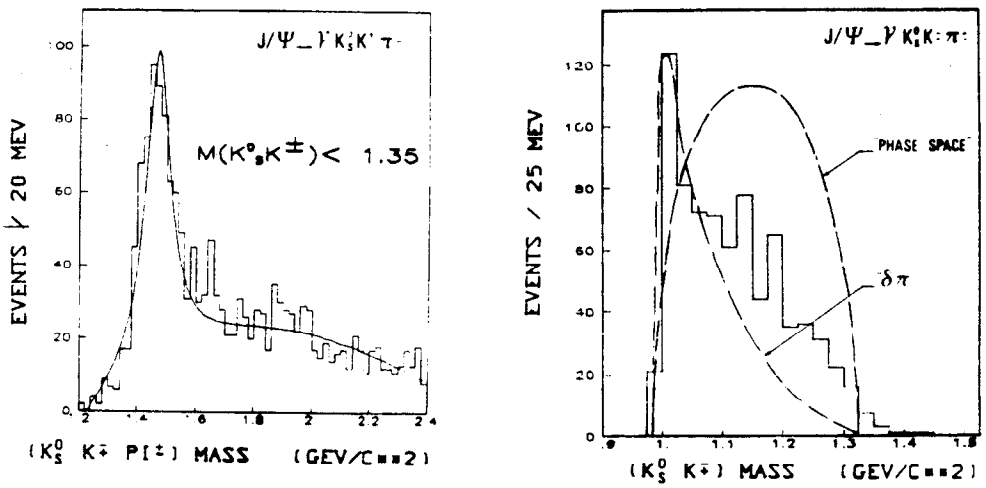

Figure 11. DM2 $\psi \to \gamma\ K_SK^\pm\pi^\mp$ [66]. **(a)** $K_SK^\pm\pi^\mp$ mass spectrum. **(b)** M($K\bar{K}$) for $1.3 < M(K_SK^\pm\pi^\mp) < 1.6$ GeV for data (histogram), and projections of $\iota \to \delta\pi$ and $K\bar{K}\pi$ phase space.

in the ι mass, but only 10±14 MeV in the width, when they impose M($K\bar{K}$) <1125 MeV.

The ι's production in radiative J/ψ decay implies C=+. Its relative branching ratios[66,74] into $K_S K^{\pm}\pi^{\mp}$, $K^+K^-\pi^0$, and $K_S K_S \pi^0$ are consistent with I=0, but also with I=1,I_3=0.

Overall I=0, C=+ limits the $K\bar{K}$ subsystem to I=1, $J^{PC} = 0^{++}(L=0)$, 2^{++}, ... The possibilities for the $K\bar{K}\pi$ total J^{PC} become for $K\bar{K}(0^{++})$: $0^{-+}(L_\pi=0)$, 1^{++}, 2^{-+}, ..., and for $K\bar{K}(2^{++})$: 2^{-+}, 1^{++}, 2^{++}, 3^{++}, ... Thus for all angular momenta 0 we would get $K\bar{K}\pi(0^{-+})$ with the $K\bar{K}$ being 0^{++}, I=1 (e.g. δ). Production of spin 1 mesons is expected to be suppressed in $\psi \rightarrow \gamma gg$, since spin 1 coupling to two massless gluons is forbidden by Yang's theorem[29]. 2^{++} is expected [78] to dominate $\psi \rightarrow \gamma gg$.

DM2 and Mark III have analyzed the spin parity of the ι with a three body helicity formalism[79], which is independent of quasi two body decays. They find consistency with $J^P(\iota)=0^-$, and Mark III[74] finds that 1^+ and 1^- have relative likelihoods $<10^{-3}$ and 10^{-6} respectively. Nobody has yet tested the possibility of spin 2.

The $K\bar{K}$ mass distribution in $\iota \rightarrow K\bar{K}\pi$ is fit much better by a δ than by phase space (Figure 11). The 0^{++} δ is a not very well understood particle. It appears as a narrow resonance in $\eta\pi$ and as a step in $K\bar{K}$. This strange behavior can be explained by its proximity to the $K\bar{K}$ threshold, and Flatté gives a two channel parameterisation of the δ[80]. However it does make the branching ratios difficult to measure, and they are not very well known[18]: $K\bar{K}/\eta\pi$= 0.25 - 4.2. It is also possible that the δ is more complicated than a normal single pole resonance[81], or that there is no δ in ι decays, but rather a final state $K\bar{K}$ interaction[82] that creates the observed low mass $K\bar{K}$ enhancement.

Upper limits for $\iota \rightarrow K^*K$ are given in Table VIII. That from Mark III is measured in the region of the Dalitz plot which is unaffected by the δ.

The 1^{++} D(1285), which also decays to $K\bar{K}\pi$, is not seen in radiative J/ψ decays; an upper limit is given in Table VIII.

4.1.2 PRODUCTION OF E → $K\bar{K}\pi$ IN HADRON COLLISIONS

The experiments which have performed spin parity analyses of $E \rightarrow K\bar{K}\pi$ are summarized in Table IX.

The first of these[67] observed $p\bar{p}$ at rest → $E\pi\pi$. They determined I=0, C=+ by comparing different charge combinations of $K\bar{K}\pi$. They observed a low mass enhancement of the $K\bar{K}$ subsystem, which prefers $J^P(K\bar{K})=0^+$. That assignment leaves $J^P= 0^-, 1^+, 2^-, \ldots$ as possibilites for the E. Comparing the first three of these to their observed mass distributions, they found 0^- prefered. The 1^{++} D(1285) was not seen in this experiment.

The most recent experiment has been performed at BNL with 8 GeV/c π^- and 6.5 GeV/c $\bar{p}$ beams[70,71]. They observe π^- p → $K_S K^{\pm}\pi^{\mp}$ n and $\bar{p}$ p → $K_S K^{\pm}\pi^{\mp}$ + anything. The E and D are both seen in both π^- and $\bar{p}$ samples.

Table IX. Spin Results on $E \to K_S K^{\pm}\pi^{\mp}$ in Hadronic Collisions.

Experiment Reference	81 cm HBC CERN 67	2 m HBC CERN 68	Ω' spectr. CERN WA76 69	MPS spectr. BNL-AGS 71, 85
Process beam energy	$p\bar{p} \to E\pi\pi$ at rest	$\pi^- p \to E\, n$ 3.95 GeV/c	$\pi^+ p \to \pi^+ E\, p$ $p\, p \to p\, E\, p$ 85 GeV/c	$\pi^- p \to E\, n$ $p\bar{p} \to E + X$ 8 GeV/c π^- 6.5 GeV/c $\bar{p}$
E mass (MeV) E width	1425±7 80±10	1426±6 40±15	1425±2 62±5	π^-: 1421±2 $\bar{p}$: 1416±5 π^-: 60±10 $\bar{p}$: 80±30
no. events in E peak background	~800 ~70	152±25 ~200	~1000 ~500	π^-: ~2000 $\bar{p}$: ~700 π^-: ~2000 $\bar{p}$: ~1400
Isospin	0	0		
$J^{PG}(E)$ for $M(K\bar{K}\pi)$	0^{-+} 1360-1460	1^{++} 1390-1470	$1^{++}(\sim 7\%\ 0^-)$ 1370-1490	0^{-+} 20 MeV bins
J^P's in fit $K\bar{K}\pi$ P.S. Flatté δ	$0^-, 1^+, 2^-$ no	$0^-, 1^{\pm}, 2^{\pm}$ yes yes	$0^-, 1^+$? yes	$0^{-+}, 1^{+\pm}, 1^{-+}$ yes yes
$E \to \delta\pi / K\bar{K}\pi$	~0.5		0.02±0.02	dominant
$E \to K^*K / K\bar{K}\pi$	~0.5	0.86±0.12	0.98	present

Table X. Partial Waves for Isobar Analysis of $K\bar{K}\pi$ and $\eta\pi\pi$.

	I	$J^{PG}=$ 0^{-+}	1^{++}	1^{+-}	1^{-+}
K^*K	0,1	P	S (D)	S (D)	P
$\delta\pi$	0,1,2	S	P	-	-
$\epsilon\eta$	0	S	P	-	-
$\epsilon\rho$	1	-	-	S	-

A Dalitz plot analysis of their π^- data with Zemach amplitudes[83] was presented last year[84]. Now a full partial wave analysis has been completed[70,71]. This is not a Dalitz plot fit; the full information is used by describing each event by two masses and three angles. In each 20 MeV $M(K\bar{K}\pi)$ bin a maximum likelihood fit is made to an incoherent background plus the $\delta\pi$ and K^*K waves

listed in Table X. The two channel parameterization of Flatté[80] was used for $\delta \rightarrow K\bar{K}$. The results are shown in Figure 12.

1^{++} (Figure 12c) is dominant at the D(1285) mass, where they say it is mostly $\delta\pi$ possibly with a considerable amount of destructively interfering K^*K. At higher masses the 1^{++} is said to be mostly K^*K. It exhibits a sharp rise at the K^*K threshold and is the dominant contribution to $K\bar{K}\pi$ above that. Note that this threshold is in the middle of the "E" bin used by most other experiments.

The 0^{-+} (Figure 12b) exhibits a peak at ~1410 MeV, and they say it makes up at least 70% of the E(1420) peak. Here $\delta\pi$ is dominant, with a significant contribution from K^*K and strong constructive interference between them (Figure 12g,h,i). The $K^*K(0^{-+})$ and interference seem to peak at slightly higher mass than the $\delta\pi(0^{-+})$.

The $K^*K(1^{+-})$ wave (Figure 12d) also shows a peak at about 1400 MeV, of the same magnitude as that in $\delta\pi(0^{-+})$. The decision as to whether the 0^{-+} or 1^{+-} is resonating depends largely on the phase differences plotted in Figure 12j-m. They are consistent with a 0^{-+} resonance with M=1402, Γ=47 MeV (shown by dotted lines in Figure 12), but due to the 0-2π wrap-around, are also consistent with smooth behavior. The relative phase motion of $K^*K(1^{++})$ and $K^*K(1^{+-})$ is smooth, indicating that either both or neither are resonant in the E region. The BNL group decide in favor of 0^{-+}.

No partial wave analysis of the BNL $\bar{p}$ data is available, but a Dalitz plot analysis has been performed[71] (Figure 13). Also here there is a 0^{-+}peak, but the 1^{+-} contribution is small and flat. The 1^{++} is about half the amplitude of the 0^{-+} at the E, but has no peak there. The larger phase space contribution is presumably due to background, which is larger in the $\bar{p}$ sample than in the π^-.

The presence of a $K^*K(1^{++})$ step in the π^- data but not in the $\bar{p}$ is consistent with the preliminary results reported at Moriond in 1984[85]. There are pronounced K^* bands in the $K\bar{K}\pi$ Dalitz plot in and above the E region for the π^- data. This indicates that at least some of the K^* in the E region is due to the background (in agreement with the 1^{++} wave measured above). The $\bar{p}$ data doesn't have K^* bands in the background region, and they may be less pronounced in the E region. (Note that K^* bands near threshold can be simulated by the kinematic motion of the δ in these plots[70].)

A puzzle is introduced by noting that a cut requiring low $K\bar{K}$ mass (which is where the K^*bands cross) strongly reduces the E peak in the $\bar{p}$ data, but not in the π^- data. The D region is only little affected in either case. The measured fractions of resonance events having M($K\bar{K}$) <1050 MeV are:

	D	E
π^- beam	0.83±0.05	0.67±0.05
$\bar{p}$ beam	0.74±0.05	0.38±0.04

Thus it seems that the "E" meson produced in π p is different than that in $\bar{p}p$, although they have the same J^P and mass. Perhaps this could be explained by interference with the background? Note that their spin analysis of the $\bar{p}$ data

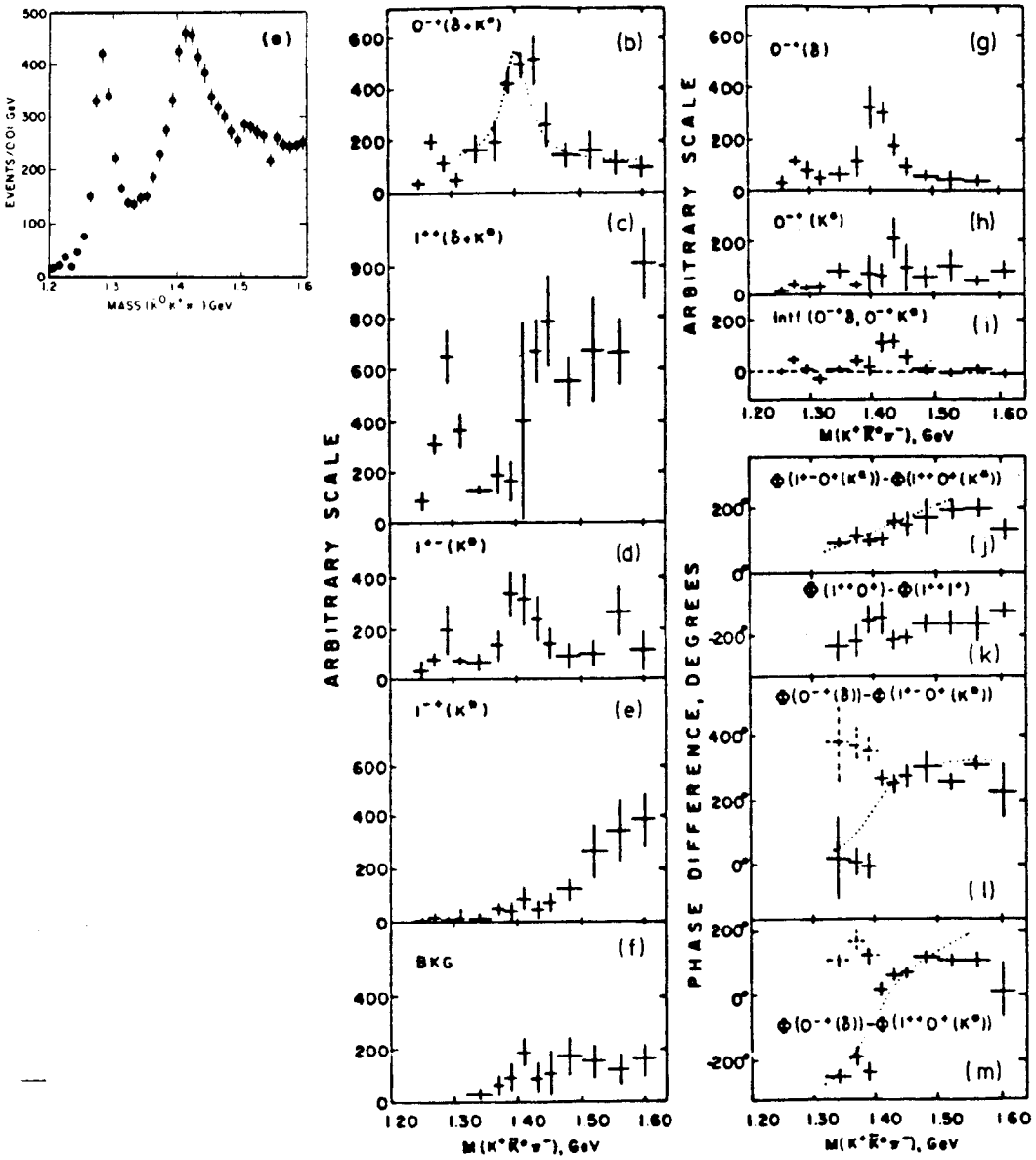

Figure 12. BNL-MPS spin parity analysis of $\pi^- p \rightarrow (K_S K^{\pm}\pi^{\mp})n$[70,71.] **(a)** full $K_S K^{\pm}\pi^{\mp}$ mass spectrum. **(b)-(h):** Acceptance corrected contributions of the labelled waves. δ stands for $\delta\pi$, and K* for K*K. **(i)** contribution of $\delta\pi(0^{-+})$ and K*K(0^{-+}) interference. **(j)-(m)** Relative phases Φ of the labelled waves. Here the notation is $J^{PG}M^{\eta}$, where M is the third component of the spin in the Gottfried Jackson frame and η is the eigenvalue of the reflection operator in the production plane.

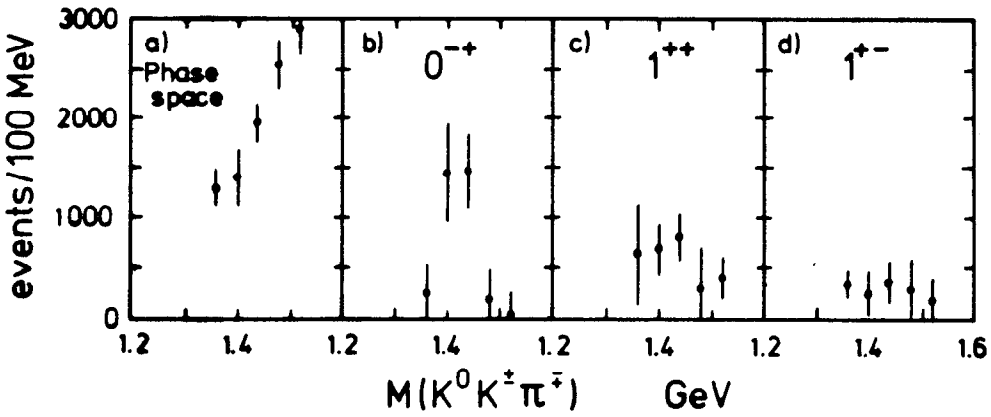

Figure 13 BNL Dalitz plot analysis of $p\bar{p} \rightarrow E + X$[71].

(Figure 13) does not extend down to the D region, so we are not sure that this is the 1^{++} D(1285) and not the 0^{-+} $\eta(1275)$[86].

Experiment WA76[69] at the CERN SPS used the Ω' spectrometer with an 85 GeV/c mixed pion and proton beam on a hydrogen target to study the exclusive reaction (π^+or p) p $\rightarrow$(π^+or p) $K_S K^{\pm}\pi^{\mp}$ p. The experiment is designed to enhance double (pomeron) exchange graphs; thus the observed $K\bar{K}\pi$ are mainly in the central region ($x_F < 0.25$). They observe peaks at the D(1285) and the E(1420), with essentially flat acceptance in this region. The p and π^+ samples show similar behavior in the Dalitz plots, so they are combined. They use an isobar model and the Zemach tensor method[83] to make maximum likelihood fits to the Dalitz plots. They test their Flatté δ parameterisation in the D region. They obtain $J^P(D) = 1^+$ and a good description of the $K\bar{K}$ mass distribution, but do not give the $\delta\pi$ and K*K fractions. For the E they perform the fit in the $M(K\bar{K}\pi)$ bin 1370 to 1490 MeV. They find the 0^- wave to be small (~7%). Assuming there is a single resonance in this bin, 1^+ is prefered over 0^- with log likelihoods 416 and 321 respectively. The 1^+ is 98% K*K, with (2±2)% $\delta\pi$.

The earlier experiment of Dionisi *et al.*[68] studying 3.95 GeV/c $\pi^- p \rightarrow (K_S K^{\pm}\pi^{\mp})$ n also found K*K(1^{++}) for the E meson, with lower statistics. In a later experiment[87] with 4.2 GeV/c K^- p $\rightarrow(K_S K^{\pm}\pi^{\mp})$ Λ they found evidence for a second K*K(1^+) resonance at 1526±6 MeV with a width of 107±15 MeV (Figure 14). They claim that this meson, which they call the D′, fits the SU(3) 1^{++} nonet better than does the E(1420). This channel favors $s\bar{s}$ meson production over $u\bar{u}$, and thus D′ over D. This 1530 resonance is an interesting candidate for the partner of the D, but needs confirmation by another experiment, preferably one at somewhat higher energy, so that the non-resonant background can be better determined. They do not mention in their paper what SU(3) assignment they want to give the E, which they observe in this experiment with about 1/4 the strength of the D′.

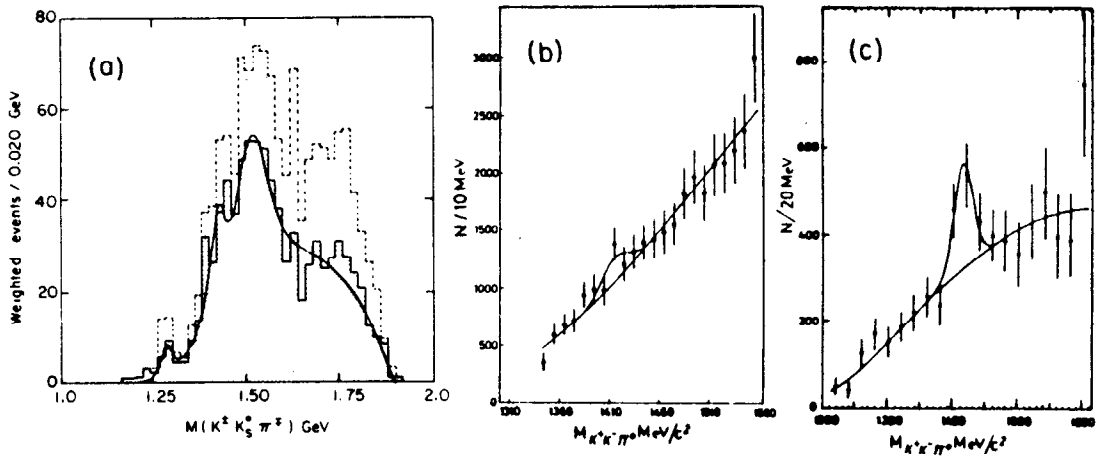

Figure 14 (a) D′ in $K^-p \to K_S K^\pm \pi^\mp \Lambda$ at 4.2 GeV/c[87]. The shaded histogram is events in forward hemisphere. The curve is fit to polynomial background + D(1270) + E(1420) + D′(1530). (b) Lepton-F upper limit for E production in $\pi^- p \to K^+ K^- \pi^0 n$ at 32.5 GeV/c[88]. (c) Lepton-F E signal in $K^- p \to K^+ K^- \pi^0 Y$ at 32.5 GeV/c.

The Lepton-F spectrometer at IHEP Serpukhov has also been used to study D and E production with π^- and K^- beams, at a considerably higher beam energy of 32.5 GeV/c[88]. They have no spin determinations, but compare production cross sections to the SU(3) expectations for 1^{++} D and E. Using the $K^+K^-\pi^0$ channel, they observe the D in their π^- data and measure

$$\frac{\sigma(\pi^- p \to En)}{\sigma(\pi^- p \to Dn)} < 0.05,$$

which restricts the D-E SU(3) mixing angle to within 13° of ideal mixing (E = pure $s\bar{s}$), if they belong to the same nonet. It is strange that the E is relatively suppressed here but produced in approximately equal rate with the D in the lower energy π^- p experiments[68,71] and in the high energy p p experiments[69,89].

They observe the E in their K^- data (again without spin determination) and measure

$$\frac{\sigma(K^- p \to EY)}{\sigma(K^- p \to En)} > 10,$$

which supports the $s\bar{s}$ assigment of the E. They do not see the D or the D′(1526).

In conclusion one must admit that confusion still reigns in the hadronically produced $E \to K\bar{K}\pi$ sector. Not all of these experiments can be right if they are all seeing the *same* E meson. (Interestingly enough, there is no controversy over the 1^{++} $\delta\pi$ nature of the D(1285)!)

The BNL experiment has some internal confusion raised by the sensitivity of the $\bar{p}$-produced E to a "δ" cut, and by the presence of a 1420 peak in the 1^{+-} partial wave. However their surprising results on the K^-K threshold, which can only be obtained by using fine $M(K\bar{K}\pi)$ binning in the partial wave analysis, demonstrates that we cannot rely on results from previous experiments which place the whole E region in one bin.

Partial wave analyses can be very tricky, since they require the data to choose between a limited set of alternatives (isobars). Perhaps none of them is right. An error in the resonance parameterisation can make the fit reject the "right" answer. Any involvement with the $\delta \rightarrow K\bar{K}$ is especially suspect, even if unavoidable. The q^{2L+1} threshold factors might not be right. It is interesting to notice that both $\delta\pi(0^-)$ and $K^-K(1^+)$ have L=0. A slight error in the efficiency can also favor one partial wave over another.

The higher statistics to be accumulated by the BNL experiment will be very welcome. Independent confirmation by another experiment with different efficiency biases is perhaps even more important. It would be interesting to see what happens to the Ω' result if the E region is divided into two bins, to either side of the K^-K step seen at BNL. For the time being, I feel we must at least be open to the possibility that the hadronically produced E has $J^{PC}=0^{-+}$.

4.1.3 SOME COMMENTS ON SU(3) CONSIDERATIONS

Arguments based on SU(3) for the 1^{++} nonet are difficult, because it is not only the E which is on shaky ground. The mesons belonging to this nonet have long been believed to be those shown in Table XI. However some measurements[90] find a considerably lower A_1 mass of 1041 MeV. The mass of the 1^{++} Q_A and the 1^{+-} Q_B depend on the mixing between the physical Q_1 and Q_2 1^+ states. Thus it si very difficult to apply the Gell-Mann Okubo meson mass formula $4M^2_{s\bar{u}} = M^2_{d\bar{u}} + 3M^2_8$, which becomes

$$4M_Q^2 = M_A^2 + 3(M_D^2 \sin^2\theta + M_E^2 \cos^2\theta).$$

More naively, if the D were pure $u\bar{u}$ and $d\bar{d}$, and the E $s\bar{s}$, one would expect the E to be about 300 MeV above the D (in good agreement with the E being replaced by the D'(1530)); mixing could reduce this difference closer to the D-E value. An SU(3) analysis which also uses the information from decay widths is performed in reference 87.

A 0^{-+} $E/\iota(1440)$ would be a candidate for the radially excited 0^{-+} nonet (Table XII) but by no means is this compelling. The other candidates for this nonet are also not very well established, and the given collection of states do not exhibit the right mass relations for an SU(3) nonet[113].

4.1.4 OTHER PRODUCTION OF $E/\iota \rightarrow K\bar{K}\pi$

Mark III has investigated[91] the channels $\psi' \rightarrow \omega\, K\bar{K}\pi$ and $\psi \rightarrow \phi\, K\bar{K}\pi$. They see a 4.6σ peak recoiling against the ω, with a mass of 1449 ± 8 and width between 18 and 100 MeV (90% C.L.). No peak is seen in the $K\bar{K}\pi$ recoiling

Table XI. Candidates for 1^{++} $q\bar{q}$ Nonet.

meson	mass	width	isospin	quark content	main decay
A_1	1275±28	316±45	1	$u\bar{d}$, etc.	$\rho\pi$
Q_A = mixture of:			1/2	$u\bar{s}$, etc.	
Q_2	1406±11	184±9	1/2	$u\bar{s}$, etc.	$K^*\pi$
Q_1	1270±10	90±20	1/2	$u\bar{s}$, etc.	$K\rho$
D	1283±5	26±5	0	$u\bar{u}, d\bar{d}$	$\delta\pi \rightarrow \eta\pi\pi$
E ?	1418±10	52±10	0	mostly $s\bar{s}$	K^*K
or D'?	1526±6	107±15	0	mostly $s\bar{s}$	K^*K

Table XII. Candidates for 0^{-+} $q\bar{q}$ Nonet.

meson	mass	width	isospin	quark content	main decay
$\pi(1300)$	~1300	200-600	1	$u\bar{d}$, etc.	$\rho\pi$
$\kappa(1350)$	~1350	~250	1/2	$u\bar{s}$, etc.	$K\pi$
$\eta(1275)$	1279±5	68±12	0	$u\bar{u}$,$d\bar{d}$,$s\bar{s}$	$\delta\pi \rightarrow \eta\pi\pi$
E/ι?	1420/1460	50/100	0	$u\bar{u}$,$d\bar{d}$,$s\bar{s}$	$\delta\pi \rightarrow K\bar{K}\pi$

against ϕ. Assuming the $K\bar{K}\pi$ state has isospin 0, they correct for the unseen charge combinations to get

$$B(\psi \rightarrow \omega\, X(1450),\ X \rightarrow K\bar{K}\pi) = (8 \pm 3 \pm 2) \times 10^{-4}$$
$$B(\psi \rightarrow \phi\, X(1450),\ X \rightarrow K\bar{K}\pi) < 2.3 \times 10^{-4}.$$

Present statistics are not sufficient for a spin parity analysis of this $K\bar{K}\pi$ signal. A $q\bar{q}$ meson which is seen with ω but not with ϕ would be expected be mostly $u\bar{u}$ and $d\bar{d}$. Therefore it is unlikely to be the traditional $s\bar{s}$ 1^{++} E (if there is one). Mark III find[91,92] that a picture of η, η', and glueball ι mixing can describe their $\psi \rightarrow$ VP data, where V = ρ, ω, ϕ, K^* and P = π, η, η', K, ι.

The JADE group at PETRA reports[93] seeing a 1490±30 MeV resonance in the channel $K_S K^{\pm}\pi^{\mp}$ in their study of ~36 GeV $e^+e^- \rightarrow$ hadrons. They have 13 events in the peak, over a background of 6 events.

Upper limits for ι production in two photon production have been set by TASSO[94] and Mark II[95] at $\Gamma_{\gamma\gamma}(\iota)$ $B(\iota \rightarrow K\bar{K}\pi) < 2.2$ (95% C.L.) and 2 keV (90% C.L.) respectively. Here we are presumably only concerned with the ι or a spin 0 E, as production of spin 1 is suppressed in two photon reactions.

4.2.1 $\psi \rightarrow \gamma\, \iota$, $\iota \rightarrow \eta\pi\pi$?

If the ι decays via $\delta\pi$, the $\eta\pi$ decay of the δ should produce a $\eta\pi\pi$ decay mode for the ι. The $\eta\pi\pi$ and $\delta\pi$ spectra shown in Figure 15 show no resem-

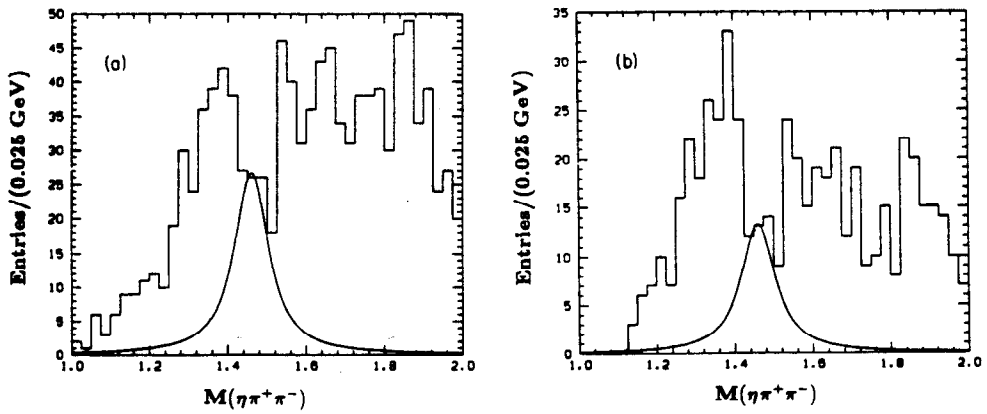

Figure 15. Mark III $\psi \rightarrow \gamma\eta\pi\pi$[74]. **(a)** M($\eta\pi\pi$) spectrum. **(b)** M($\eta\pi\pi$) for $\eta\pi$ in δ region. The curves were used to calculate the upper limits in Table VIII.

blance to the $K\bar{K}\pi$ spectra of Figure 11. The corresponding upper limits for $\iota \rightarrow \delta\pi \rightarrow \eta\pi\pi$ are given in Table VIII. More statistics have now been accumulated by Mark III, and there is still no sign of the ι[91].

However it is dangerous to make too strong conclusions on the basis of one mass region of a spectrum when we have no understanding of the neighboring regions. Other resonances, such as the $\eta(1275)$[86,96] and an enhancement at 1700 MeV[75] could be contributing and generating interference terms. If the ι and the $\eta(1275)$ are both radially excited $q\bar{q}$ mesons, they would be expected to have roughly comparable strengths in radiative J/ψ decay. It is also possible that the $\iota \rightarrow \eta\pi\pi$ decay occurs via two channels, $\delta\pi$ and $\epsilon\eta$, which interfere destructively. (Here ϵ stands for the elusive I=0, $J^{PC}=0^{++}$ $\pi\pi$ resonance at ~600-800 MeV.) These questions can't be answered until a partial wave analysis has been made of the $\psi \rightarrow \gamma\ \eta\pi\pi$ channel.

4.2.2 HADRONIC PRODUCTION OF E $\rightarrow \eta\pi\pi$?

The reaction π^- p $\rightarrow \eta\pi^+\pi^-$ n was studied at 8.45 GeV/c by Stanton *et al.*[86] at the Argonne AGS. They detected the $\eta \rightarrow \gamma\gamma$ and the π^+ and π^-. The $\eta\pi$ mass plots show a significant δ signal for M($\eta\pi\pi$) in the D region (1220-1320 MeV), and little δ elsewhere.

They made a phase shift analysis using the $\epsilon\eta$, $\rho\eta$, and $\delta\eta$ isobars. Spins larger than 1 were found not to be needed. The background from non-η events was <17%, and was well described by the $\epsilon\eta(0^-)$ wave. The analysis was done in 100 MeV bins, except for a few narrower bins near the D.

The I=0 $\delta\pi(1^+)$ wave (Figure 16a) has a sharp peak and rapid phase variation at the D(1285), and is practically 0 elsewhere. Note that experiments which have seen a 1^{++} E meson observed it in K*K, not in $\delta\pi$, so it would not necessarily appear in this spectrum.

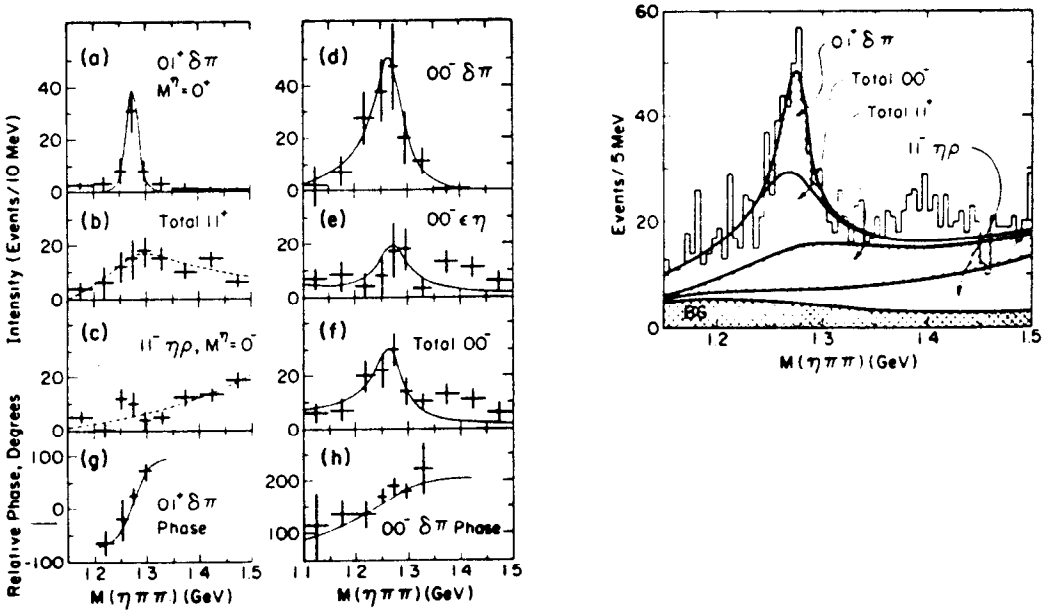

Figure 16. AGS Partial wave analysis of π^- p $\rightarrow$ ($\eta\pi^-\pi$) n$^{(86)}$. **(a-f)** Intensities of the labeled partial waves. The notation is IJ^P. Note the lack of data points in (d) above 1400 MeV. **(g)** Relative phases of I=0 and I=1 for $\delta\pi(1^+)$. **(h)** Relative phases of $\delta\pi$ and $\epsilon\eta$ for I=0 J^P=0 . (i) Total $\eta\pi^+\pi^-$ data compared to sum of D, $\eta(1275)$, 1^-, and 1^- curves drawn in (a)-(f).

The I=0 $\delta\pi(0^-)$ has a broader peak at ~1275 MeV with a width ~70 MeV. This peak, which has become known as the $\eta(1275)$, is seen with less significance in I=0 $\epsilon\eta$. The two waves are negatively interfering in this range, so that the total 0^- is smaller than the $\delta\pi(0^-)$ alone. The 0^- and 1^+ waves seem to be incoherent, suggesting that the D and $\eta(1275)$ are produced in different nucleon helicity states. The $\eta(1275)$ production in the $\eta\pi^+\pi^-$ final state is about 3 times that of the D in that state.

There is no sign of a peak at 1420 in $\delta\pi(0^-)$, but actually there are no points drawn above 1400 MeV for that wave (Figure 16d,h). There may be a signal in $\epsilon\eta(0^-)$, and the total $\eta\pi^+\pi^-$ spectrum has an indication of a peak at ~1400 MeV, which is not explained by the sum of the waves.

The same reaction has recently been studied with similar statistics by Ando *et al.*[96] at at KEK. Their beam energy is nearly the same (8 GeV/c) and they also detect the $\eta\to\gamma\gamma$. The $\eta\pi\pi$ mass spectrum shows a clear peak at 1280 MeV, and a hint of structure near 1400. A "δ" cut (950 <M($\eta\pi$) <1010 MeV) retains the structure but reduces the background (Figure 17).

Upon performing a partial wave analysis in 20 MeV M($\eta\pi\pi$) bins to $\delta\pi(0^-,1^+)$, $\epsilon\eta(0^-,1^+)$, $\rho\eta(1^+,1^-)$, a more complicated picture emerges.

The I=0 $\delta\pi(1^+)$ spectrum shows a peak and rapid phase variation at 1280 MeV. The mass and width are in good agreement with those of the 1^{++} D meson[18].

The I=0 $\delta\pi(0^-)$ spectrum has two clear peaks, one at the position of the $\eta(1275)$ and the other at the E. The masses are 1279±5 and 1420±6 MeV respectively. The widths, which still include the ~20 MeV experimental resolution, are 64±22 and 31±26 MeV. Strong phase motion is observed at both masses.

The $\epsilon\eta(0^-)$ contribution is large but jagged. The total I=0 0^- spectrum has no peak at 1.42! This is because the $\delta\pi$ and $\epsilon\eta$ exhibit strong destructive interference in this region. (Here the effect has been measured, whereas it was only hypothesised as an explanation for the nonappearance of the ι in $\psi\to\gamma\eta\pi\pi$.)

High statistics results on π^-p $\to$ ($\eta\pi^0\pi^0$) n at 100 GeV/c have been presented at this conference by the GAMS collaboration[97]. Their $\eta\pi^0\pi^0$ spectrum has a peak at 1420 MeV (Figure 18a) for events with large t (-t>0.1 GeV/c^2). When events in the E region are selected, the $\eta\pi^0$ mass plot shows a clear δ peak (Figure 18b). Their 1420 peak in the total spectrum is larger than those of the previous two experiments. The difference might be due to the prohibition of $\eta\rho$ in this charge state. GAMS has not yet done a partial wave analysis, so can say nothing about the spin contents of their peaks.

The WA76 Ω' spectrometer experiment, whose $J^P=1^+$ determination for E$\to$K$\bar{K}\pi$ was described above, has also analysed (π^+or p) p $\to$ (π^+or p) $\eta\pi^+\pi^-$ p at 85 GeV/c[98] (Figure 19). Their η decays into $\pi^+\pi^-\pi^0$, with the π^0"seen" as missing mass. The missing mass plot does show a clear π^0 peak, with signal to background better than 1 to 1. But the combinatorics make the η peak

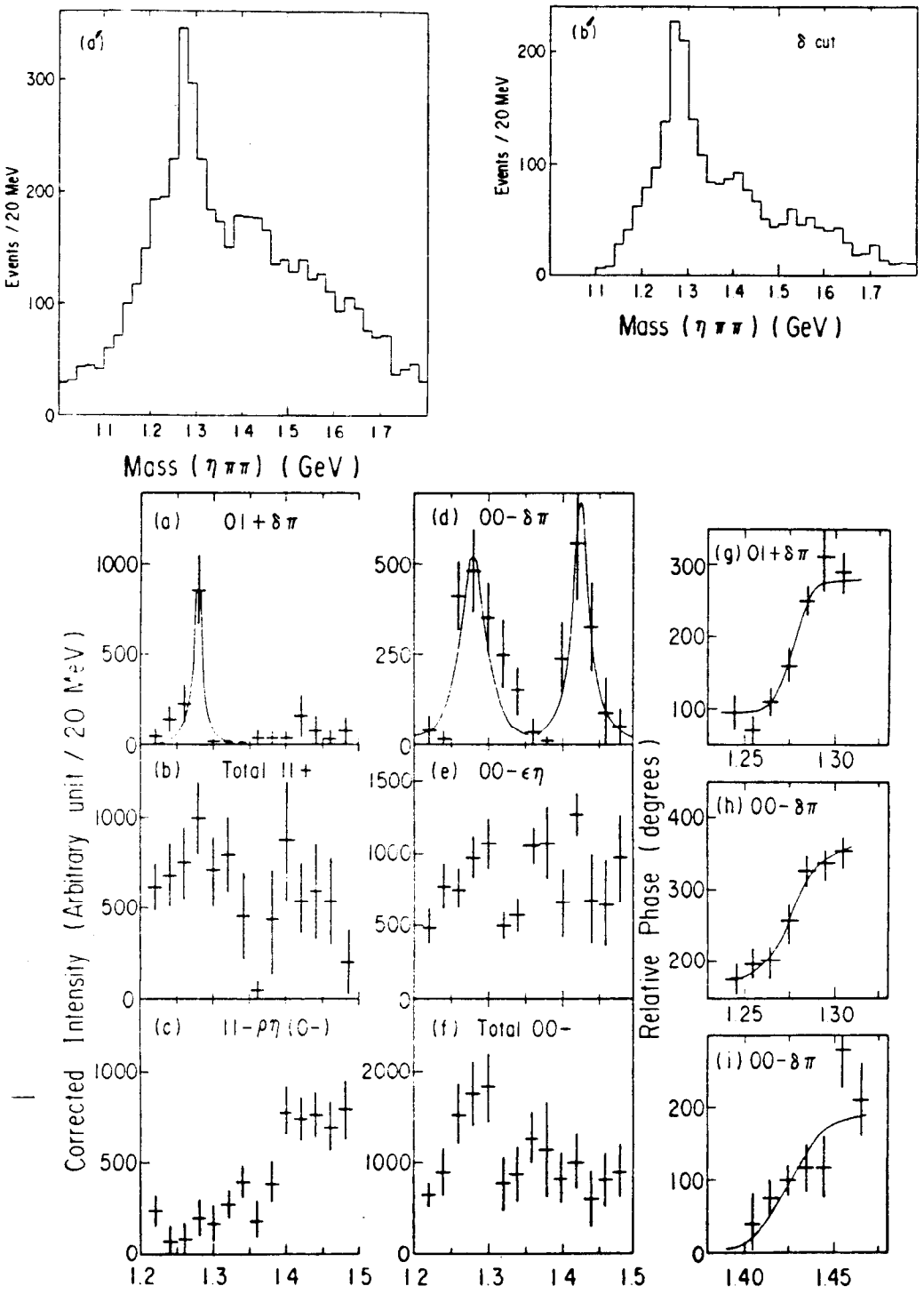

Figure 17. KEK Partial wave analysis of $\pi^- p \to (\eta\pi^+\pi^-)\, n^{(90)}$. **(a')** Full $M(\eta\pi\pi)$ spectrum. **(b')** $M(\eta\pi\pi)$ for $950 < M(\eta\pi) < 1010$ MeV. **(a)(f)** Intensity distributions of labeled waves. **(g)-(i)** Phase variations of labeled waves relative to $\rho\eta(0^-)$.

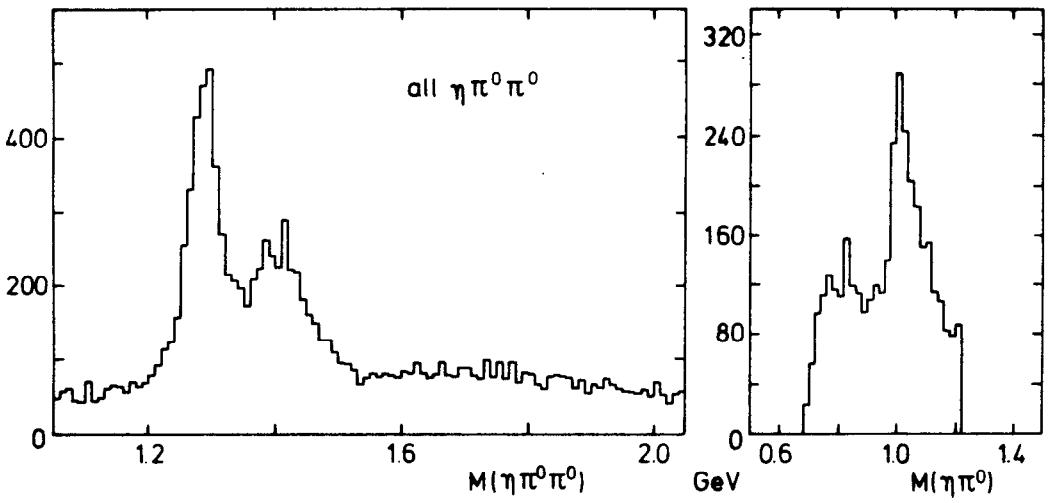

Figure 18 GAMS[97] $\pi^- p \rightarrow \eta\pi^0\pi^0$ n. (a) $M(\eta\pi^0\pi^0)$ for events with -t>0.1 GeV and with $A_2\pi^0$ and $f\eta$ events removed. The peaks are also evident without this last cut. (b) $M(\eta\pi^0)$ for events in E region of (a).

in the $M(\pi^+\pi^-\pi^0)$ spectrum nearly invisible without background subtraction. The $\eta\pi^+\pi^-$ spectrum is made by taking as η all $\pi^+\pi^-\pi^0$ combinations with mass between 510 and 590 MeV, and weighting with the inverse of the number of combinations. It is unclear how much background results from this process. The final $\eta\pi^+\pi^-$ spectrum is similar to that of KEK. However the result of the phase shift analysis is completely different. WA76 sees the D and perhaps the E in $\delta\pi(1^{++})$, but nothing in any $\delta\pi(0^-)$ or any other 0^- channel. No $\eta(1275)$. No $E/\iota(1420)$.

Majority vote seems to favor the $\eta(1275)$ and a $0^-(1420)$ in the $\eta\pi\pi$ channel. Unfortunately nothing more definite can be said at this time. I will discuss possible differences due to production mechanisms in section 4.4, where I also compare $K\bar{K}\pi$ to $\eta\pi\pi$.

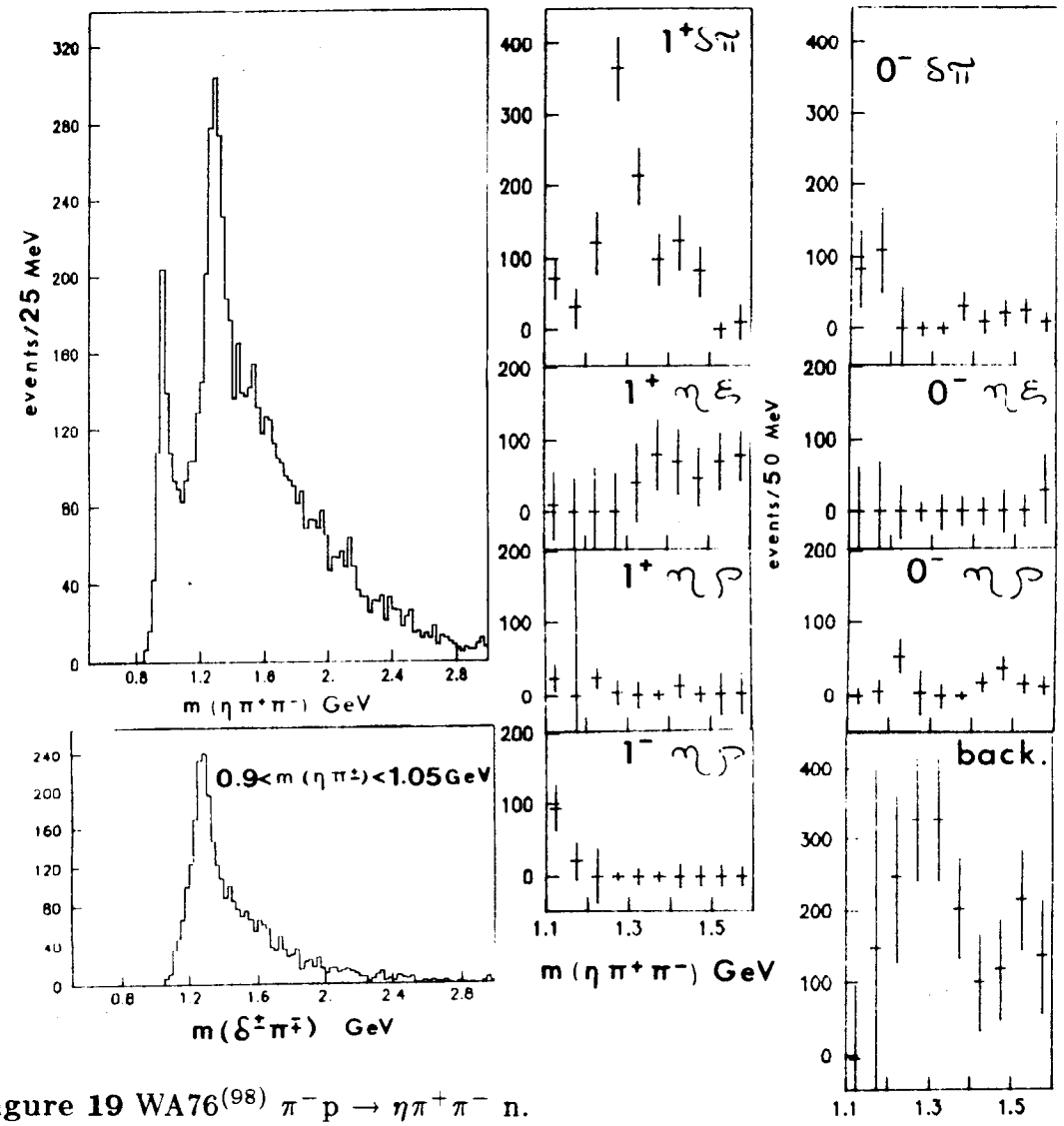

Figure 19 WA76[98] $\pi^- p \rightarrow \eta\pi^+\pi^- n$.

4.3.1 $\overline{\psi} \rightarrow \gamma\iota$, $\iota \rightarrow \gamma\rho$?

A $\gamma\rho$ decay of a pure glueball would be surprising, but a relatively small $q\bar{q}$ admixture would be sufficient to give a respectible branching ratio.

The experimental results on $\iota \rightarrow \gamma\rho$ are confusing. Crystal Ball[99], DM2[66], and Mark III[74] have all seen a $\gamma\rho$ peak in radiative J/ψ decays, but at ~1400 MeV and with a shoulder towards lower masses (Figure 20). Mark III has shown (section 4.3.4) that phase space effects alone cannot account for such a mass shift. However, other particles may be contributing to this spectrum besides the $\eta'(958)$ and the ι, for example the $\eta(1275)$ or f(1270). Fits with three resonances give a good description of the data, as shown in Figure

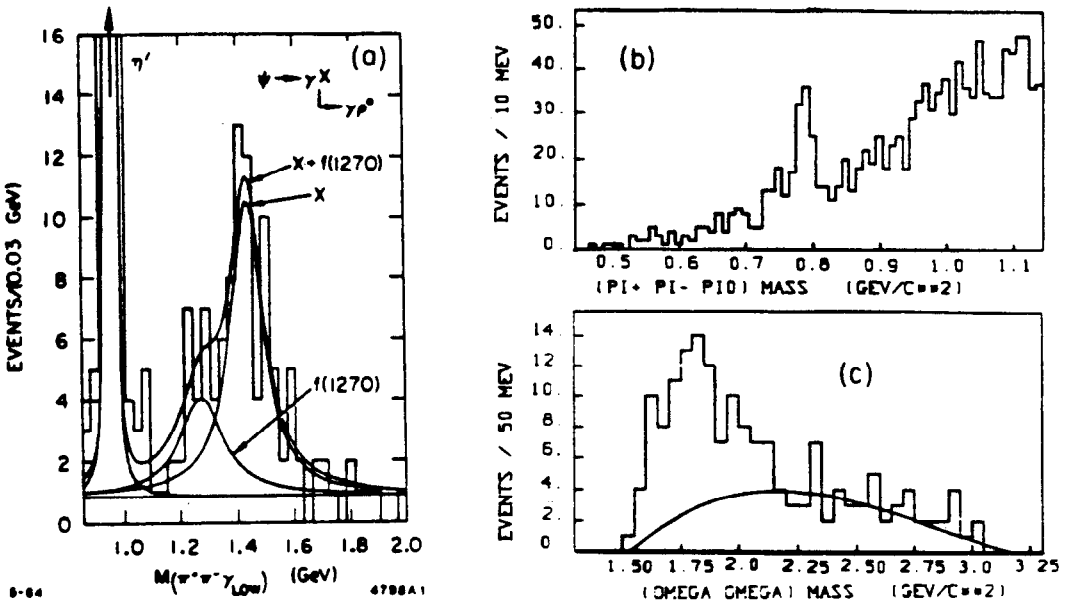

Figure 20. (a) Mark III $\psi \to \gamma + \gamma\rho$[74]. Fit of $\gamma\rho$ spectrum with f(1270) + X gives X mass 1434 MeV. (b) DM2 $\psi \to \gamma\omega\omega$[66]. ω signal in $\pi^+\pi^-\pi^0$ mass plot of $\gamma + 6\pi$ events when other $\pi^+\pi^-\pi^0$ is selected to be in ω region. (c) $\omega\omega$ mass spectrum. Curve is background estimated from ω sidebands.

Table XIII. $\psi \to \gamma$ X, X $\to \gamma\rho$.

	Crystal Ball	Mark III	DM2
References	99	74	66
Fits with only one resonance X			
X Mass (MeV)	1390 ± 25		1401 ± 18
X Width (MeV)	185^{+110}_{-80}		174 ± 44
number of events in X peak	61 ± 15		123 ± 20
$B(\psi \to \gamma X, X \to \gamma\rho) \times 10^4$	$1.9 \pm 0.5 \pm 0.4$		$0.9 \pm 0.2 \pm 0.14$
Fits with $\eta(1275)$ + X			
X Mass (MeV)	1440 (fixed)	1434 ± 14	
X Width (MeV)	55 (fixed)	133 ± 32	
number of events in X peak	29 ± 7	77 ± 15	
$B(\psi \to \gamma X, X \to \gamma\rho) \times 10^4$	$0.9 \pm 0.3 \pm 0.2$	$1.1 \pm 0.2 \pm 0.3$	
$B(\psi \to \gamma\iota, \iota \to \gamma\phi) \times 10{-}4$		< 1.6	
$B(\psi \to \gamma\iota, \iota \to \gamma\omega) \times 10{-}4$		< 2.3	

20. The branching ratios and masses obtained from these fits are summarized in Table XIII. One should note that the fits neglect interference effects, which might shift the ι mass further.

Table XIV. $\psi \to \gamma VV$

VV	Mass Range in GeV	J^P	$B(\psi \to \gamma VV) \times 10^3$	Peak (MeV)	Experiment
$\rho^0\rho^0$	<2	all	(1.3±0.5)	1650±50	Mark II[100]
$\rho^+\rho^-$	1500-1900 1700 peak	all	(mostly 0^- or 2^- (3±1)	1700±40	Crystal Ball[99]
$\rho\rho$	<2	all	(6.2±1.5)	1550, 1800	Mark III[101]
	<2	0^-	(5±1)	~1600	
$\omega\omega$	all	all	1.8±0.1±0.5	~1800	Mark III[106]
	<2	all	1.2±0.1±0.3		
	<2	0^-	1.0±0.4		
$\omega\omega$	all	all	0.8±0.2±0.2	~1800	DM2[66]
$\phi\phi$	<2.8	all	0.31±0.04±0.06		DM2[66]

The spin parity analysis of the $\gamma\rho$ signal is difficult. The spin one case has free parameters which can be adjusted to give angular distributions identical to spin 0 in two of the three angles, and the third suffers from acceptance problems[74]. The observed distributions are *consistent* with $J^P=0^-$; more cannot be concluded without much better statistics.

At present the connection between the $\gamma\rho$ enhancement and the ι is suggestive but not compelling.

4.3.2 $\psi \to \gamma\ \rho\rho$

The decay $\psi \to \gamma\rho^0\rho^0$ was first observed by Mark II[100]. The $\rho\rho$ mass distribution was dominated by a peak at mass 1650±50 and width 200±100 MeV. This was at first thought to be associated with the 2^{++} state $\Theta(1710)$.

The Mark III group[101] has now analysed the $\psi \to \gamma\ \pi^+\pi^-\pi^+\pi^-$ and $\psi \to \gamma\ \pi^+\pi^0\pi^-\pi^0$ decays from a sample of 2.7 $\times 10^6$ J/ψ events. The two channels show similar 4π mass distributions, which are summed in Figure 21a. Two peaks are clearly evident at ~1550 and ~1800 MeV, above a background which is due mostly to 5π events with an undetected π^0 decay γ. A clear $\rho\rho$ peak is evident in the $\pi^+\pi^-$ and $\pi^\pm\pi^0$ channels, but not in the wrong sign combinations.

Mark III[102]and Crystal Ball[99] have shown that the angle χ between the two ρ decay planes shows the characteristic[103] $1 - \cos 2\chi$ distribution for even spin odd parity. This also rules out the association of the $\rho\rho$ enhancement with the Θ, and also with the low mass enhancement seen[104] in $\gamma\gamma \to \rho^0\rho^0$ which has been shown[105] to be *not* predominantly odd parity.

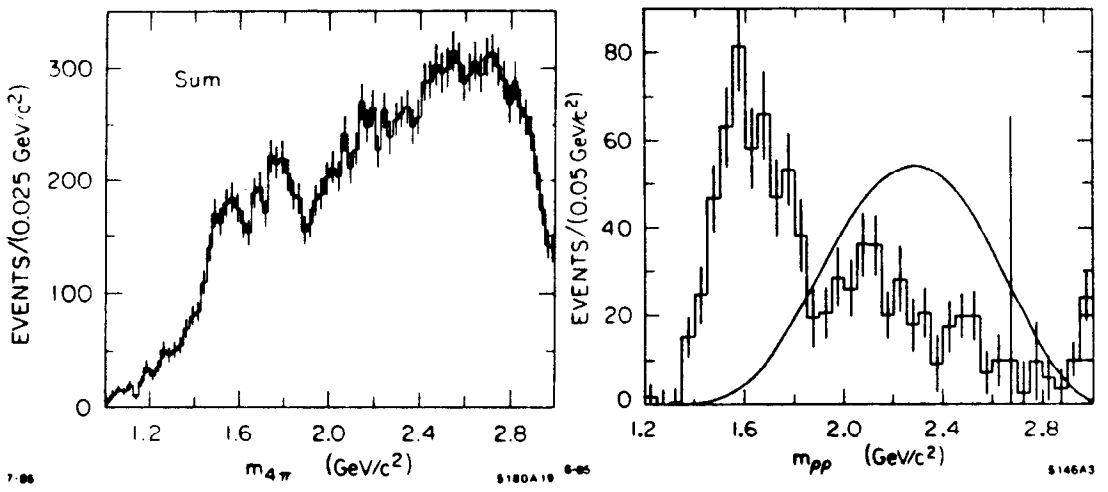

Figure 21. (a) Mark III $\psi \to \gamma 4\pi$ unsubtracted 4π mass spectrum (sum of $\pi^+\pi^-\pi^+\pi^-$ and $\pi^+\pi^0\pi^-\pi^0$). (b) The 0^- $\rho\rho$ component. The curve is $\psi \to \gamma\rho\rho$ P wave phase space.

Mark III[101] has now performed a maximum likelihood fit to the 10 channels:

$\rho\rho$ states of $J^P = 0^+, 0^-, 1^+, 1^-, 2^+, 2^-$,
isotropic 4π, isotropic $\rho\pi\pi$, isotropic $\rho\rho$,
$A_2\rho$ where $A_2 \to \rho\pi$ and a π is missed.

The fit shows the spectrum to be dominated by isotropic 4π and 0^- $\rho\rho$. The 0^- $\rho\rho$ mass distribution is shown in Figure 21b, compared to that expected from non resonant P wave $\rho\rho$. A clear enhancement is seen centered at ~1600 MeV. Considering the uncertainties introduced by this type of fit, they consider it consistent with the two peak structure seen in 4π, but it seems more likely to be associated with the ~1550 MeV peak.

4.3.3 $\psi \to \gamma\ \omega\omega$

Both Mark III[106] and DM2[66] (Figure 20) have observed $\psi \to \gamma\omega\omega$ and applied the decay plane analysis described above to show that the $\omega\omega$ is predominantly 0^- or 2^-. Mark III has also performed a fit allowing 0^-, 0^+, 1^-, 1^+, 2^-, 2^+, and isotropic $\omega\omega$, and found that the $\omega\omega$ is $(85 \pm 19)\%$ 0^-.

4.3.4 THE "PSEUDOSCALAR PUZZLE" IN RADIATIVE J/ψ DECAYS

After observing radiative J/ψ decay 0^- enhancements in

$K\bar{K}\pi$	at 1460 MeV	0^{-+}
$\gamma\rho$	at 1400 MeV	consistent with 0^-
$\rho\rho$	at ~1600 MeV	0^-
$\omega\omega$	at ~1800 MeV	0^-
$\eta\pi\pi$	at 1380 MeV	unknown J^P

the Mark III group has tested the hypothesis[107] that they are all manifestations of the ι.

They describe[64] the ι with a coupled channel Breit Wigner[108] which includes the effects of unitarity and the opening of the various decay

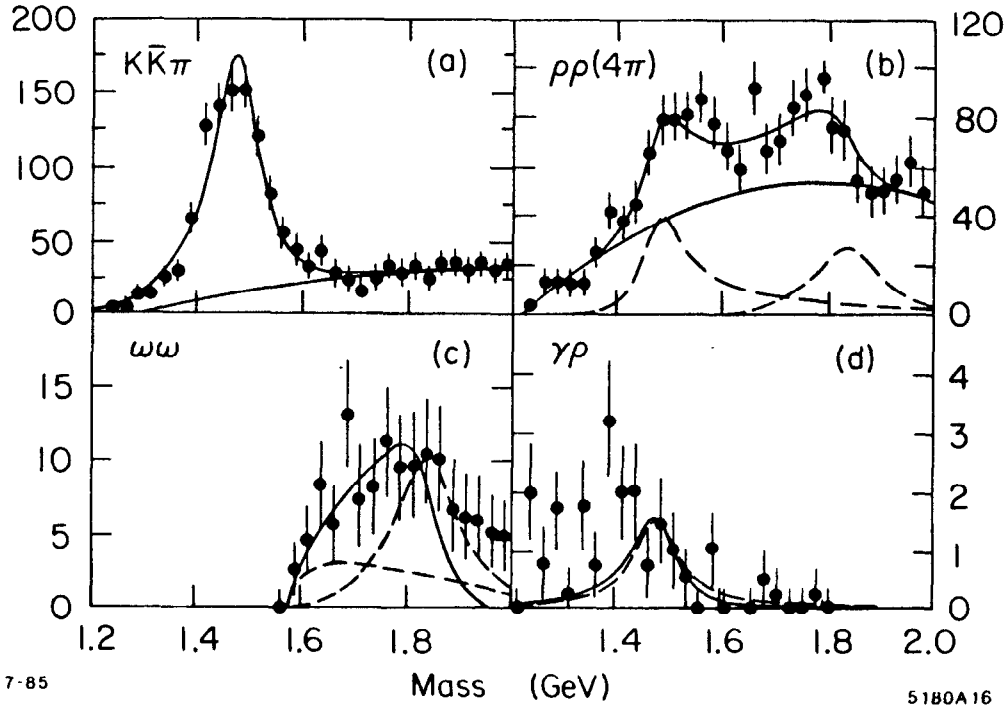

Figure 22. MarkIII coupled channel fit for $\psi \rightarrow \gamma X$, to the following 4 decay channels of the 0^- X: (a) Sum of $K^+K^-\pi^0$ and $K^0_S K^\pm \pi^\mp$. (b) $\pi^+\pi^-\pi^+\pi^-$ with 5π backgound subtracted. (c) Background subtracted $\omega\omega$. (d) Background subtracted $\gamma\rho$. The fit assumes that the "ι" is coupled to $K\bar{K}\pi$, $\rho\rho$, $\gamma\rho$, and $\omega\omega$. A second resonance is introduced to fit the ~1800 MeV peak in the $\rho\rho$ distribution, and is coupled also to $\omega\omega$ and $\gamma\rho$. The solid curves indicate the total result of the fit, and in (a) and (b) also the fitted background. The dashed curves indicate the resonance contributions. In (c) negative interference makes the total less than the sum of the two resonances above 1800 MeV. In (d) the dashed curve is the ι; the full curve adds the small contribution from the 1800 MeV resonance.

channels with increasing mass. The fit is shown in Figure 22.

Phase space pushes the "ι" peak in the $\rho\rho$ channel up high enough to fit the ~1550 MeV peak in the 4π distribution. (I suspect the fit would not be as good if they had chosen to use their extracted 0^- $\rho\rho$ mass distribution of Figure 21.) A second resonance at ~1800 MeV is included to describe the second peak observed in the 4π spectrum. It is assumed not to couple to $K\bar{K}\pi$, but must by SU(3) appear in the $\omega\omega$ spectrum. In fact, according to the fit, it is the dominant contribution to $\omega\omega$.

The $\omega\omega$ distribution below 1800 MeV is well fit by the two constructively interfering resonances, but that curve is well below the data above 1800 MeV, where the interference is negative. SU(3) predicts that the coupling to $\rho\rho$ should be 3 times that to $\omega\omega$; the fit gives 5.0 ± 0.7.

The effects of phase space are minimal for the $\gamma\rho$ channel and fail to move the "ι" peak down from 1460 to the 1400 MeV peak in $\gamma\rho$. However possible efects of the $\eta(1275)$ are not included in this fit. The fit shown has the $\rho\rho$ coupling 3300 ± 600 times that of $\gamma\rho$, while $\sim$400 is expected from VDM.

The poorly understood $\eta\pi\pi$ spectrum is the only one left entirely out in the cold.

The relative success of this analysis is perhaps more appealing than the spectre of 4 unrelated 0^- resonances in the 1.4 - 2 GeV region. Perhaps further refinements can improve the it. The interested reader should study reference 64 for full details on the fit described here. This analysis is based on MarkIII's old 2.7 million J/ψ sample. They now have 3 million more, and DM2 has 8.6 million J/ψ's which could be analysed in this way.

4.4 THE E/ι PUZZLE

The ι is certainly one of the most intriguing things to have come out of J/ψ decays. If the Mark III hypothesis described in the last section is right, they get a $\psi\rightarrow\gamma\iota$ branching ratio of at least 0.7%. This is a substantial fraction of the total expected $\psi\rightarrow\gamma$gg rate of about 9%. Something that is produced so strongly in radiative J/ψ decays should be able to teach us something about gluons, whether it is a glueball itself or not. The quark model needs a radially excited 0^{-+} state in the general area of 1400 MeV. If there is also a 0^{-+} gluonium state near there, the two could hardly help but mix. Then our ι would contain both gg and $q\bar{q}$, and it would be surprising if it were not produced in both radiative J/ψ decays and hadronic processes. The gg and $q\bar{q}$ parts of it might be produced with different strengths in the two reactions, and differently in hadronic reactions depending on the beam particle and kinematic conditions (pomeron exchange or whatever). The mixing hypothesis raises another question: when two particles mix, they form two new particles. Where is the second 0^{-+} particle? Is there one at 1440 MeV and another one somewherelse, or is one at 1420 and the other at 1460? The ι has been puzzling us for 5 years now, and I suspect will continue for another 5. But if we want to understand gluonium and gluon coupling to hadrons, it is one of the better places to look.

It may be possible to bring some sense into the hadronic collisions data by paying attention to the different type of reactions.

If π^- p $\rightarrow$ X n is mediated by the exchange of one particle in the t channel, that particle must have I=1. If one pion exchange dominates, the nucleon spin must flip and the π must have L=1 relative to the nucleon. On the other hand, for the simplest case where the exchanged particle has no angular momentum and the nucleon spin state does not change, the exchanged particle will be I=1 $J^P=0^+$, i.e. the δ. Then one has $\delta\,\pi$ scattering at the other vertex, and should not be to surprised to produce a $\delta\pi$ resonance if there is one. In the $K\bar{K}\pi$ final state we have two experiments of this type. The low statistics one (Dionisi

et al.[68]) at 4 GeV/c gets $K^*K(1^{++})$ for the E, but the high statistics BNL experiment[71,84] at 8 GeV/c gets $\delta\pi(0^-)$. For $\eta\pi\pi$ we have Stanton *et al.*[86] at 8.5 GeV/c which see both $\delta\pi(1^{++})$ and $\delta\pi(0^{-+})$ at 1280 MeV and don't say much about 1400 MeV. The KEK experiment[96] is at nearly the same energy, agrees with Stanton *et al.*, and adds the $\delta\pi(0^-)$ peak at 1420 MeV.

π^+ p $\rightarrow$ π^+ X p at high energies where the π^+ goes forward in the final state and the p backward is very different from the previous reaction. The usual diagram is double Pomeron exchange, i.e. the π^+ and p both emit a Pomeron, and the two Pomerons meet to produce the system X. (The Pomeron has I=0 and $J^{PC}=0^{++}$and thus could not be exchanged in π^- p $\rightarrow$ X n.) WA76[69,98] provides the only spin-analysed $K\bar{K}\pi$ and $\eta\pi\pi$ data in this reaction, and sees only 1^{++} at the positions of the 0^- $\eta(1275)$ and $E/\iota(1440)$. The Pomeron is often thought to be multiple gluons, and double Pomeron scattering to be especially suited to making glueballs. Therefore it is rather disappointing that this is the reaction where the ι has not been seen. Nonetheless, it is a different reaction from π^- p, and one should not be surprised if it makes different particles.

$p\bar{p}$ is yet another type of reaction, and I cannot discover any particular similarity it has to π^- p or to π^+ p. Here we have two experiments: Baillon *et al.*[67] with $p\bar{p}$ annihilation at rest and the BNL experiment with 6.5 GeV/c $p\bar{p}$[85]. Both see 0^{-+} at 1420 MeV.

Thus we can accomodate almost all of the hadronic collisions data mentioned here, at the expense of having two particles at 1420 MeV: a 0^{-+} which is produced in π^-p and decays to $K\bar{K}\pi$ and $\eta\pi\pi$ via $\delta\pi$, and a 1^{++} which is produced in $\pi^+$and decays to K^*K.

The radiative J/ψ data wants to add to this an interference effect which eats the $\eta\pi\pi$ decay mode of the $0^{-+}$and shifts its mass and width up by 40 MeV. Or else a third particle at 1460 MeV, which then needs interference to eat its $\eta\pi\pi$ decay or new KK final state interactions to fake the $\delta\pi$ in its $K\bar{K}\pi$ decay mode. This third particle could be mostly glueball, with the other two mostly $q\bar{q}$ and belonging to the 1^{++} and radially excited 0^{-+} nonets.

5. THE Θ

The Θ was first observed by the Crystal Ball[109] as an $\eta\eta$ resonance at 1640 ± 50 MeV of width 220^{+100}_{-70} MeV in radiative J/ψ decays. Subsequent measurements by Mark II[110], Mark III[63], and DM2[66] of $\psi\rightarrow\gamma K\bar{K}$ have shown two peaks in this region. The first corresponds to the f'(1525). The second is the Θ at 1711 ± 8 MeV with a width of 147 ± 13 MeV. The resonance parameters in Table XV are all from fits to non-interfering f' and Θ. Mark III has shown[63] that the Θ parameters are not significantly changed by including interference. The Crystal Ball $\eta\eta$ spectrum could be described by the $\Theta(1710)$ and the f'[40], if the $f'\rightarrow\eta\eta$. Or perhaps by the Θ and the 0^{++} $G(1590)\rightarrow\eta\eta$ seen by GAMS[111].

The most intriguing aspect of the Θ comes from the spin analyses. In $\psi \rightarrow \gamma + K\bar{K}$ or $\pi\pi$, only $J^{PC} = 0^{++}, 2^{++}, \ldots$ are allowed. For J=0 the

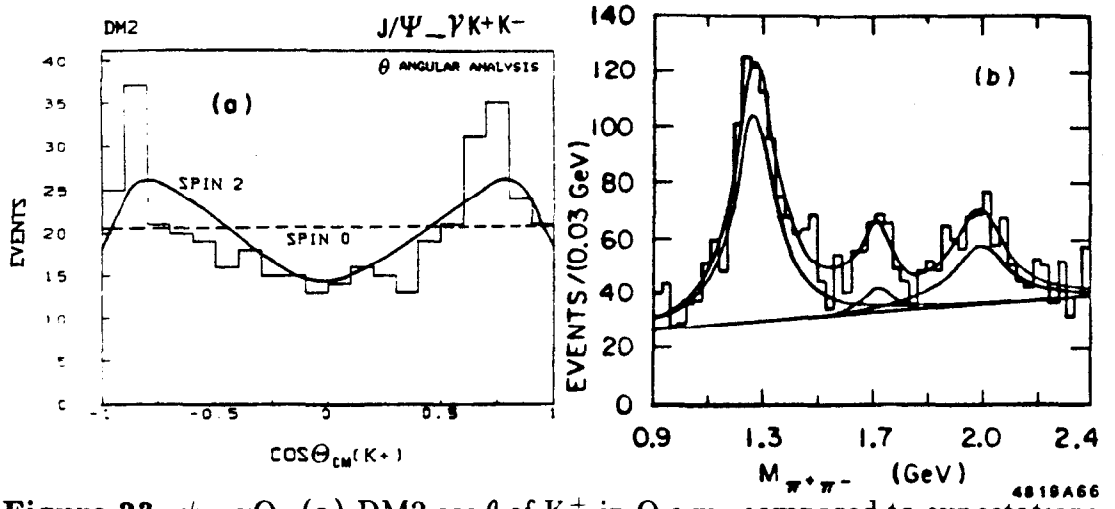

Figure 23. $\psi \to \gamma\Theta$. **(a)** DM2 $\cos\theta$ of K^+ in Θ c.m. compared to expectations for spin 0 and 2. **(b)** Mark III[63] fit to $\pi\pi$ mass spectrum with interfering f, f′, and Θ. The top curve is the total fit. The lower curves are the three individual resonance contributions and the flat background.

angular distributions are completely determined. For J = 2 they depend on the (complex) helicity amplitudes A_0, A_1, A_2 for helicity 0, ±1, ±2. Thus the helicity parameters x, y, ϕ_x, ϕ_y

$$x e^{i\phi_x} \equiv \frac{A_1}{A_0}, \qquad y e^{i\phi_y} \equiv \frac{A_2}{A_0}$$

must be included in the fit. In the Mark III analysis[63] J(Θ)=2 is prefered over 0 at the ~99.9% C.L. A small mystery is that the J=2 solution has a smaller likelihood than expected from Monte Carlo simulations. DM2[66] only obtains a significant preference for spin 2 if they fix $\phi_x = \phi_y = 0$.

The surprise comes from the helicity amplitudes (Table XV), which indicate approximately equal production of helicity 0, 1, and 2 for the Θ. This is very different from the nearby 2^{++} f and f′, where helicity 2 is surpressed. Here the Θ seems to not be behaving like its $q\bar{q}$ neighbors! (But one should also note that the f and f′ do not obey the expectation[112] for qq of x ~ y >0.5!)

The Θ's large rate in radiative J/ψ decay, along with the lack of a place for it in a 2^{++} $q\bar{q}$ nonet, have lead to speculation that it is a glueball or other strange object. Donoghue has said[113] "it is almost certainly our first state to be identified as non $q\bar{q}$."

To enhance its status as a glueball candidate, the Θ would do well to exhibit flavor-independent decay ratios. An SU(3) singlet should have[114] couplings $K\bar{K}$:$\eta\eta$:$\pi\pi$= 4:1:3, which become 6:1:12 after phase space effects are included. Therefore everybody has looked for $\Theta \to \pi\pi$, with dubious success. There is a danger of fitting a fairly flat spectrum with a succession of peaks.

Table XV. Properties of Θ in Radiative J/ψ Decay.

The quoted $K\bar{K}$ results are all from fits to the f′(1525) + Θ. The $\pi\pi$ spectra were fit to f(1270) + Θ+ X(~2100). Interference was neglected in both cases; it could substantially reduce the $\pi\pi$ branching ratios[63]. The branching ratios assume I=0, C=+ for the Θ, thus $K\bar{K} = \frac{1}{2}K^+K^- + \frac{1}{4}K_SK_S + \frac{1}{4}K_LK_L$ and $\pi\pi = \frac{2}{3}\pi^+\pi^- + \frac{1}{3}\pi^0\pi^0$. All masses are in MeV. Upper limits are 90% confidence level.

	Crystal Ball	Mark II	Mark III	DM2
References	109, 40	110	63, 101	66
N(Θ)	20±6	~50	192±25	410
Mass(Θ)	fixed†	1700±30	1720±10±10	1707±10
Width(Θ)	fixed†	156±20	130±20	166±33
Spin 2 Helicity Amplitudes:				
x,y Θ	fixed†	1.2±.6, -.9±.6	-1.1±.2,-1.1±.3	-1.3±.1,-1.1±.2
x,y f′	fixed†		0.6±.1, 0.2±.2	1.1±.1, 0.2±.1
x,y f	.9±.1, .0±.2	0.8±.2, 0.0±.2	1.0±.1, 0.1±.1	
ϕ_x,ϕ_y Θ	fixed†		0.6±.8, -0.1±.5	0.±1.4, 1.3±.3
ϕ_x,ϕ_y f′	fixed†		1.3±.6, 2.6±.9	-2.6±.3,-4.2±.4
ϕ_x,ϕ_y f	0,0 (fixed)		-0.5±.7, 0±2	
Branching ratios ×10⁴				
$\psi\to\gamma\Theta$, $\Theta\to\eta\eta$	2.6±0.8±0.7			
$\psi\to\gamma\Theta$, $\Theta\to K\bar{K}$		12±2±5	9.6±1.2±1.8	9.2±1.4±1.4
$\psi\to\gamma f'$, $f'\to\eta\eta$	1.9±0.8±0.5			
$\psi\to\gamma f'$, $f'\to K\bar{K}$		1.8±0.6±1.0	6.0±1.4±1.2	5.0±1.2±0.8
$\psi\to\gamma\Theta$, $\Theta\to\pi\pi$	2.3±0.7±0.8	<3.2	2.4±0.6±0.5	1.8±0.3±0.3
$\psi\to\gamma\Theta$, $\Theta\to\rho\rho$			<5.5	
$\psi\to\gamma\Theta$, $\Theta\to K^*K^*$			<4.5	

† fixed at Mark III values for f′ + Θ fit.

Although everybody quotes branching ratios, most do not discuss the statistical or other significance of their signals. The f(1270) is clearly present, with perhaps a shoulder due to the f′(1525). There seems to be an enhancement at ~2100 MeV, which could be the h(2030). The space between the f′ and the 2100 can be well described by the Θ. Since at least the first three of these resonances have the same quantum numbers 2^{++} they can interfere. This has not yet been allowed for in the branching ratios quoted in Table XV. Mark III[63] has preformed a fit with all resonances interfering, with the surprising result that the "Θ" bump is mainly caused by f′ and X(2100) interference, substantially decreasing the real $\Theta\to\pi\pi$ contribution to the plot (Figure 23).

Perhaps the equality does not apply to the $K\bar{K}$, $\pi\pi$, etc. couplings, but

o the $u\bar{u}$, $d\bar{d}$, and $s\bar{s}$. Then one needs to compare ($K\bar{K}$+ $K\bar{K}\pi$+ ...) to ($\pi\pi$ + 4π+ $\rho\rho$ + ...). I think no spin analysis of a 4π final state is possible, so we have a lot of freedom to hypothesis $\Theta \rightarrow u\bar{u}$ branching ratio there. The $\rho\rho$ enhancement has been shown[101] to be dominantly not 2^{++} Θ, but the upper limit given in Table XV is not too stringent.

Some evidence for hadronic production of the Θ is starting to appear. Although the results so far are very tentative and of questionable statistical significance, I will describe them briefly since this is an important line of investigation that may teach us about mechanisms of glueball formation.

DM2[66] observes $\psi \rightarrow K\bar{K}\phi$. The $K\bar{K}$ mass spectrum is dominated by the f′, with a shoulder at ~1640 MeV. A fit with the f′ interfering with the $\Theta(1710)$ is also possible. Their $\psi \rightarrow K_S K_S \phi$ spectrum is rather different. Here the f′ and Θ appear with about equal strengths, and the Θ is at its proper mass. For both the Θ and the f′ the branching ratio $\psi \rightarrow \phi\, K\bar{K}$ are $(4\pm1) \times 10^{-4}$.

WA76[98] observes (π^+ or p) p $\rightarrow$ (π^+ or p) $K\bar{K}$ p at 85 GeV with the $K\bar{K}$ being centrally produced ($|x_F| < 0.3$). The K^+K^- spectrum shows the f′ and peaks at 1630±10 and 1730±20.

GAMS[111] has done a partial wave analysis of π^- p $\rightarrow \eta\eta$ n at 100 GeV. In spin 2 they observe f, f′, and something at 1.8-2.0 GeV. There is no evidence for the Θ, at a level of <20% of the rate for their 0^{++} gluonium candidate G(1590).

TASSO[94] gives a limit on Θ production in two photon reactions of $\Gamma_{\gamma\gamma}(\Theta)$ $B(\Theta \rightarrow K\bar{K}) < 0.28$ keV (95% C.L.). This is not yet sensitive enough to compare to their corresponding value for the f′ which is 0.11±0.02±0.04 keV.

6. THE $\phi\phi$ RESONANCES

Lindenbaum *et al.*[115] measure π^- p $\rightarrow \phi\phi$ n at 22 GeV/c using the BNL MPS spectrometer. The $\phi\phi$ signal (~4000 events) is strongly dominant over the Zweig-allowed 4K or $\phi K\bar{K}$. This reaction is especially well suited to partial wave analysis because the ϕ is a narrow and the background is small (~13%). The exclusive reaction and two ϕ spins provide additional analysing power, allowing a unique solution even when all 52 waves up to L=3,J=4 are included. The 2^{++} waves dominate the $\phi\phi$ channel near threshold. The best fit (Figure 24a) is achieved with three 2^{++} resonances, which they name g_T:

$M = 2050^{+90}_{-50}$	$\Gamma = 200^{+160}_{-50}$ MeV	mostly L=0, S=2
$M = 2300^{+20}_{-100}$	$\Gamma = 200^{+60}_{-50}$	mostly L=2, S=2
$M = 2350^{+20}_{-30}$	$\Gamma = 270^{+270}_{-130}$	mostly L=2, S=0.

The background waves are too small to be used as a reference to check the phase motion across these resonances. Comparing the 2^{++} waves among themselves, one sees strong phase motion of the L=2,S=0 wave relative to the L=0,S=2. The two S=2 waves are fairly constant relative to each other. They have now analysed the $\phi K\bar{K}$ background as a check, and find only 7% 2^{++} there.

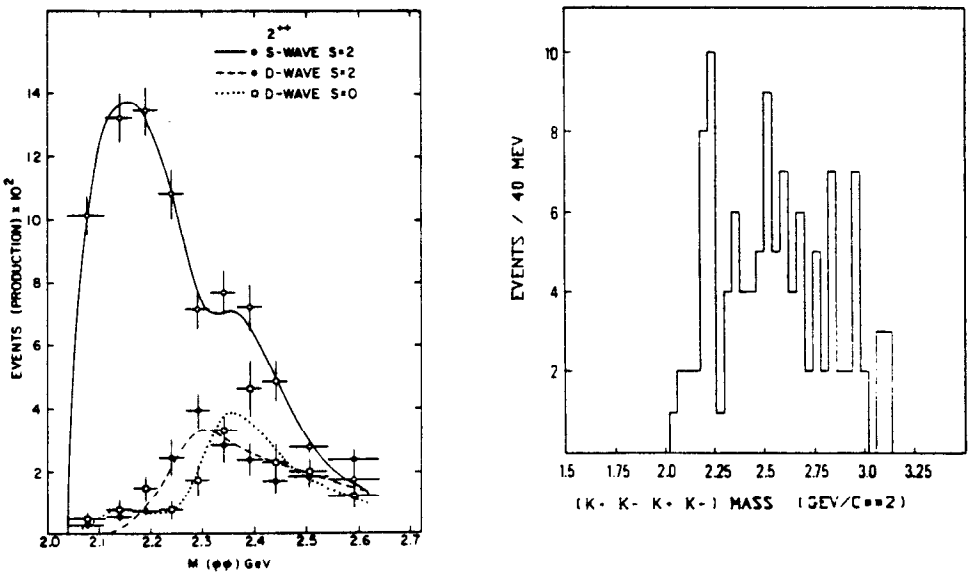

Figure 24 (a) 2^{++} waves in π^- p $\rightarrow \phi\phi$ n[115]. (b) DM2 $\psi \rightarrow \gamma\, \phi\phi$[66].

Experiment WA67[116] used the Ω spectrometer to measure π^- Be $\rightarrow$ $\phi\phi$+ X at 85 GeV/c. They have accumulated 34 000 candidate $\phi\phi$ events using triggers designed to enhance central production. Therefore they limit their analysis to angular distributions which are independent of the production process. This means that they are unable to separate S and D waves. They confirm the large $\phi\phi$ enhancement between 2.0 and 2.5 GeV. Trying fits of this region to single spin parity states, they find that 2^{++} gives the best agreement.

Lindenbaum *et al.* claim that since production of $\phi\phi$ should be strongly Zweig surpressed in their reaction, they must be seeing glueballs. There is considerable controversy (References 113, 117, 118, 119, 120) on this point. Nevertheless it is clear that this $\phi\phi$ effect is an interesting candidate for something new. If it is our best glueball candidate, why aren't we more excited? I think it is because it has so far been seen in only one type of production reaction, and, what's worse, in only one decay channel. That makes it very hard to learn anything from it. The $\phi\phi$ channel is favored experimentally because it is very clean and the ϕ spins help the partial wave analysis. Nevetheless I think it is important to look for other decay channels. Even upper limits would give us something to think about, if they came near to the $\phi\phi$ rate.

Lindenbaum *et al.*[121] have measured π^- p $\rightarrow$ $K_S K_S$ n with the same apparatus. They have performed a partial wave analysis and see no evidence for the g_T particles, but give no upper limit.

Mark III[106] give an upper limit for $\omega\omega$ production in radiative J/ψ decay of B($\psi \rightarrow \gamma\, \omega\omega$) $<2.6 \times 10^{-4}$ for the $\omega\omega$ mass range 2.1-2.4 GeV. Their corresponding limit[101] for $\rho\rho$ is $<6.0 \times 10^{-4}$.

DM2[66] may have seen something in $\psi \rightarrow \gamma\phi\phi$. The $\phi\phi$ mass distribution

shown in Figure 24b might have a peak at ~2.2 GeV, which could be one of the g_T's, or the ξ. The statistical significance is disappointing, especially when one considers that this plot comes from 8.6 million ψ decays. At 2.2 GeV their efficiency is about 10%. The total branching ratio for $\psi \rightarrow \gamma\phi\phi$ with M($\phi\phi$) <2.8 GeV is $(3.1 \pm 0.4 \pm 0.6) \times 10^{-4}$.

7. THE η AND π^0 WIDTHS

The η and π^0 widths are very fundamental numbers. That of the η is especially important in the light of the many recent attempts to assign gluon content to the η' by studying η/η' mixing.

The η width to two photons has been previously measured using the Primakoff effect, in which the η is formed from an incoming photon beam interacting with a virtual photon of the Coulomb field of a heavy nucleus. The η is then detected via its decay to $\gamma\gamma$, and its angular distribution relative to the beam axis is plotted. The cross section for η production in the Coulomb field has been calculated, and is proportional to $\Gamma^{\eta}_{\gamma\gamma}$. η's can also be produced in the hadronic field of the nulceus. The two contributions can be statistically separated by fitting the angular distributions, since that for production in the Coulomb field is peaked at smaller angles. The systematics of this separation are checked by comparing results from different beam energies and different targets. The first such experiment[122] suffered from uncertainties in the separation of the Coulomb and hadronic amplitudes. The second experiment, performed in Cornell[123] is believed to have succeeded in this separation, and quotes a very small error: $\Gamma^{\eta}_{\gamma\gamma} = 0.324 \pm 0.046$ keV.

Now results are available from several two photon experiments, which measure $e^+e^- \rightarrow e^+e^-\gamma\gamma$, $\gamma\gamma \rightarrow \eta \rightarrow \gamma\gamma$. In order to measure $\Gamma^{\eta}_{\gamma\gamma}$, these experiments rely on calculations of the "two photon flux", essentially the $e^+e^- \rightarrow e^+e^-\gamma\gamma$ part of the reaction. They must also subtract any possible background from beam-gas production of η's, i.e. $ep \rightarrow \eta + X$. The four measurements available agree with each other quite well (Table XVI). Two of them have errors approaching that of the Primakoff experiment. Together they give an average of 0.56 ± 0.04, which is a factor of 1.7 larger than the Primakoff result.

Additional two photon experiments are not likely to resolve the conflict, since we already have several and they all agree with each other. In order to check that the two photon flux calculation is right in this mass range one could measure $e^+e^- \rightarrow e^+e^-e^+e^-$. This has not been explicitly done at low masses. Mark II[124] have shown that $\gamma\gamma \rightarrow \pi^+\pi^-$ makes up only a small fraction of the two charged particle final state below the f(1270). Their measured rate for $\gamma\gamma \rightarrow$ two charged particles agrees well with the calculations for $\gamma\gamma \rightarrow e^+e^- + \gamma\gamma \rightarrow \mu\mu$. Although no number is given, it looks like a decrease of 1.7 in the $e^+e^- + \mu\mu$ rate would require a $\pi\pi$ contribution much larger than what they have measured with their identified π's.

Both the Primakoff and two photon techniques can be "calibrated" at the π^0. By far the most accurate measurement of the π^0 lifetime has been

Table XVI. π^0 and η Width Measurements.

$\Gamma(\eta\to\gamma\gamma)$ (keV)		
(1.0±0.2)†	Primakoff	Bemporad *et al.*[122,18]
0.32±0.05	Primakoff	Browman *et al.*[123]
0.56±0.16	Two Photon	Crystal Ball (SPEAR)[125]
0.58±0.02±0.06 (prel.)	Two Photon	Crystal Ball (DORIS)[126]
0.53±0.04±0.04	Two Photon	JADE[127]
0.64±0.14±0.13	Two Photon	TPC/PEP-9[128]
0.56 ± 0.04	Two Photon	average
$\Gamma(\pi^0)$ (eV)		
7.3±0.2±0.1	Decay Length	Cronin *et al.*[129]
7.9±1.4±1.6 (prel.)	Two Photon	Crystal Ball[130]
12±1	Primakoff	Bellettini *et al.*[131]
7.3±0.6	Primakoff	Kryshkin *et al.*[132]
8.0±0.4	Primakoff	Browman *et al.*[123]
$\Gamma(\eta')$ (keV)		
4.3±0.3	Two Photon	average[133]

† Not included in average because uncertainty from separation of Coulomb and hadronic amplitudes has apparently been underestimated[18]

made recently by Cronin *et al.*[129] at CERN. Their accuracy was achieved by using high energy π^0's with a mean decay length of $\sim 50\mu$m, and measuring this decay length with a clever multi-target technique. Their result is in good agreement with previous experiments, including the Primakoff experiment of Browman *et al.*, who also measured the η. However one should note that in the π^0 case Browman *et al.* have less background under the π^0 and better fits to the angular distributions than they achieved for their η experiment. The π^0 experiment also included some "off-axis" data, which enabled them to better check the production rate in the hadronic field.

The Crystal Ball collaboration is attempting to test the two photon technique by measuring the π^0. If there were an error in the two photon method which caused the difference between the two photon and Primakoff η width, it would have to be a factor of $\frac{560\pm 40}{324\pm 46} = 1.7\pm 0.3$. If this same error factor applied to the π^0, Crystal Ball would expect to measure that factor times the Cronin π^0 width, or 13±2 eV. Their preliminary result (Table XVI) is barely in agreement with this, but in excellent agreement with the result of Cronin *et al.* This measurement is based on a few weeks' run with a special trigger. Considerably more data is being taken during this summer. The systematic error quoted for the preliminary result can also be reduced substantially by more Monte Carlo statistics.

Pending clarification of the η width problem, I shall refrain from discussing the $\eta/\eta'/gg$ mixing question.

8. CONCLUSIONS

In summary, mesons made out of heavy quarks are well behaved, and lighter mesons are confusing.

The experimental and theoretical controversies in $b\bar{b}$ spectroscopy have cleared away, and the spectrum is well described by the potential model, with asymptotic freedom incorporated at short distances, and confinement of the $b\bar{b}$ via effective scalar particle exchange. The hadronic widths of $b\bar{b}$ mesons agree fairly well with QCD, but more work is needed to make a quantitative test. Measurements in $p\bar{p}$ annihilation have yielded widths and precise masses for the χ_c states, and possibly the first evidence for the elusive $^1P_1$ state. All these measurements could be improved with more statisitics and better detectors. The forecast on the theoretical side is more uncertain, and the need greater. Now that we seem to understand $Q\bar{Q}$ mesons, we can test the same ideas on $Q\bar{q}$ mesons. Data is now available on the B^*, F^*, and D^{**}.

The search for glueballs has been fascinating and frustrating us for several years. New this year are possible $\rho\rho$, $\omega\omega$, and $\gamma\rho$ decay modes of the $J^{PC}=0^{-+}$ $\iota(1460)$ seen in radiative J/ψ decays. More data on the $\psi \rightarrow \gamma\ \eta\pi\pi$ still doesn't show a sign of the ι; a spin parity analysis might help. There is some evidence for production of either the E or the ι in $\psi \rightarrow \omega\ K\bar{K}\pi$ and in jet fragmentation. The E(1420), previously believed to be a 1^{++} $q\bar{q}$ meson, has now become quite controversial. A new high statistics experiment measuring $\pi^- p \rightarrow K\bar{K}\pi\ n$, and another measuring $\pi^- p \rightarrow \eta\pi\pi\ n$ both have evidence for a $J^{PC}=0^{-+}$ meson at 1420 MeV. This might be the same particle as the $\iota(1460)$, if the 40 MeV mass and width differences could be explained away. These experiments do not see the 1^{++} E(1420), which is however seen by a high statistics $\pi^+ p \rightarrow \pi^+\ K\bar{K}\pi\ p$ experiment. The apparent discrepancy might be due to the wide $M(K\bar{K}\pi)$ bin used by this last experiment. Or perhaps it is seeing a different 1420 resonance because it is studying a different production reaction. The people involved in the hadronic experiments need to get together to make careful comparisons of their data and analysis methods before we can decide whether the E and ι are one, two, or three particles.

The Θ remains unexplainable as a $q\bar{q}$ resonance. Gluonium advocates want it to have a $\pi\pi$ decay, but the experimental data is inconclusive due to the complexity of the $\pi\pi$ spectrum in radiative J/ψ decay. A spin parity analysis has not yet been done. There may be first signs of Θ production in hadronic reactions.

The g_T $\phi\phi$ resonances are still with us, but there is a lack of new experimental information, which makes it difficult to learn much about gluonium here at this time.

Even our old friendly $q\bar{q}$ mesons are managing to confuse us: Primakoff and two photon experiments disagree by a factor of 1.7 on the η width.

ACKNOWLEDGMENTS For their help in preparing and checking this paper, I thank Elliott Bloom, Kay Brockmüller, Wilfried Buchmüller, Bob Clare, Kay Königsmann, Helmut Marsiske, Michael Peskin, David Williams, and all the speakers of the parallel sessions on Heavy and Light Spectroscopy at Bari.

REFERENCES

1 K. Han *et al.*(CUSB), Phys. Rev. Lett. 49 (1982) 1612;
G. Eigen *et al.*(CUSB), Phys. Rev. Lett. 49 (1982) 1616.

2 J. Lee-Franzini (CUSB), Proc. 5^{th} Int. Conf. on Physics in Collision, Autun,France, July 1985. See also: C. Klopfenstein *et al.*(CUSB), Phys. Rev. Lett. 51(1983)160; F. Pauss *et al.*(CUSB), Phys. Lett. 130B(1983)439.

3 A. W. Nilsson (ARGUS), talk in session P08 of this conference; H. Albrecht *et al.*(ARGUS), DESY 85-068, submitted to Phys. Lett.

4 D. Peterson (CLEO), Proc. Int. Conf. on Hadron Spectroscopy, College Park, Maryland, April 1985. See also: P. Haas *et al.*(CLEO), Phys. Rev. Lett. 52(1984)799;

5 R. Nernst *et al.*(Crystal Ball), Phys. Rev. Lett. 54 (1985) 2195; W. Walk *et al.*(Crystal Ball), contributed paper to session P08 of this conference.

6 T. Appelquist, H. D. Politzer, Phys. Rev. Lett. 34 (1975) 43; A. De Rújula, S.L.Glashow, p. 46; and all four, p.365. E. Eichten, K. Gottfried, T. Kinoshita, J. Kogut, K. D. Lane, T.-M. Yan, p.369.

7 H.B. Henriques, B.H. Kellet, R.G. Moorhouse, Phys. Lett. 64B(1976)85.

8 J. L. Richardson, Phys. Lett. 82B (1979) 272.

9 F. L. Feinberg, Phys. Rev. Lett. 39 (1977) 316, Phys. Rev. D17 (1978) 2659; W. Fischler, Nucl. Phys. B129 (1978) 157.

10 S. Gupta and S. Radford, Phys. Rev. D24 (1981) 2309 and D25 (1982) 3430; and with W. W. Repko, Phys. Rev. D26 (1982) 3305, Phys. Rev. D30 (1984) 2424, Phys. Rev. D31 (1985) 160, Wayne State Univ. Preprint WSU-Th (1985) sub. to Phys. Rev. D.

11 H. Schnitzer, Phys. Rev. Lett. 35 (1975) 1540;
J. Pumplin, W. Repko, A. Sato, Phys. Rev. Lett. 35(1975)1538.

12 D.Gromes, Nucl. Phys. B131(1977)80.

13 E. Eichten and F. Feinberg, Phys. Rev. D23 (1981) 2724.

14 W. Buchmüller, Phys. Lett. 112B (1982) 479.

15 D. Gromes, Zeit. Phys. C26(1984)401; and Lectures given at the Yukon Advanced Study Institute, Whitehorse, Yukon, August 1984, Heidelberg preprint HD-THEP-84-2?.

16 J. Baake, Y. Igarashi and G. Kasperidus, Zeit. Phys. C9 (1981) 203.

17 M. Campostrini, talk in session P08 of this conference; C. Michael Proc. Rencontre de Moriond, Les Arcs, March 10-17, 1985; S. W. Otto and J. D. Stack, Phys. Rev. Lett. 52 (1984) 2328.

18 Particle Data Group, Rev. Mod. Phys. 56 (1984)

19 A. Martin, Phys. Lett. 93B (1980) 338.

20 W. Buchmüller, G. Grunberg, S-H. H. Tye, Phys. Rev. Lett. 45 (1980) 103, 587. W. B., S.-H. H. Tye, Phys. Rev. D24 (1981) 132. W. B., Moriond Workshop on Heavy Flavors, Les Arcs, Jan. 24-30, 1982.

21 P. Moxhay, J. L. Rosner, Phys. Rev. D28 (1983) 1132.

22 R. McClary and N. Byers, Phys. Rev. D28 (1983) 1692.

23 M. Bander, D. Silverman, B. Klima, U. Maor, Phys. Rev. D29 (1984) 2038.

24 K. Königsmann, DESY 85/089, Proc. 5^{th} Int. Conf. on Physics in Collision, Autun, France, July 1985.

25 T. Skwarnicki (Crystal Ball), Proc. Rencontre de Moriond, Les Arcs, March 10-17, 1985; DESY 85-042.
26 M. G. Olsson, A. D. Martin, A. W. Peacock, Phys. Rev. D31 (1985) 81.
27 The potentials used are listed in W. Walk (Crystal Ball) paper contributed to session P09 of this conference, and inRef. 24.
28 R. Barbieri, R. Gatto, R. Kögerler, Phys. Lett. 60B (1976) 183.
29 L. D. Landau, Soviet Physics "Doklady" 60 (1948) 207. C. N. Yang, Phys. Rev. 77 (1950) 242.
30 R. Barbieri, R. Gatto, Phys. Lett. 61B (1976) 465.
31 The principle of the calculation is well described in R. Barbieri *et al.*, Nucl. Phys. B154 (1979) 535. The results for the P states are in R. Barbieri *et al.*, Phys. Lett. 95B (1980) 93 and Nucl. Phys. B192 (1981) 61.
32 M. Peskin, private communication.
33 P. B. Mackenzie, G. P. Lepage, Phys. Rev. Lett. 47 (1981) 1244.
34 S. J. Brodsky, G. P. Lepage, P. B. Mackenzie, Phys. Rev. D28 (1983) 228.
35 E. Eichten, K. Gottfried, T. Kinoshita, K. D. Lane, T. M. Yan, Phys. Rev. D21 (1980) 203.
36 L. Bugge (R704) talk in session P08 of this conference, and contributed paper by C. Baglin *et al.*
37 J. E. Gaiser (Crystal Ball), Ph.D. Thesis. SLAC-255, August 1982.
38 E. D. Bloom, C. W. Peck, Ann. Rev. Nucl. Part. Sci. 33 (1983) 143.
39 M. Oreglia *et al.*(Crystal Ball), Phys. Rev. D25 (1982) 2259. M. J. Oreglia (Crystal Ball), Ph.D. Thesis, SLAC-236, Dec. 1980.
40 R. A. Lee (Crystal Ball), PhD thesis, SLAC-282 (1985)
41 A. De Rújula, H. Georgi, S. L. Glashow, Phys. Rev. D12 (1975) 147.
42 A. Duncan, Phys. Rev. D13 (1976) 2866.
43 Early evidence included the following states. Those marked with † do not exist; but when you read older theory papers it is useful to know that they once were thought to.
X(2800)†: W. Braunschweig *et al.*(DASP), Phys. Lett. 67B (1977) 243.
W. D. Apel *et al.*(Serpukhov), Phys. Lett. 72B (1978) 500.
$\chi_c(3415)$: G.J.Feldman *et al.*(SLAC-LBL)Phys. Rev. Lett. 35(1975)821.
$\chi_c(3455)^\dagger$: J.S.Whitaker *et al.*(SLAC-LBL)Phys. Rev. Lett. 37(1976)1596
$P_c(3510)$: W. Braunschweig *et al.*(DASP), Phys. Lett. 57B (1975) 407.
$\chi_c(3555)$: J.S.Whitaker *et al.*(SLAC-LBL)Phys. Rev. Lett. 37(1976)1596.
$P_c(3590)^\dagger$: W. Bartel *et al.*, Phys. Lett. 79B (1978) 492.
44 $\eta_c(2980)$: R. Partridge *et al.*(Crystal Ball), Phys. Rev. Lett. 45 (1980) 1150; T. Himmel *et al.*(SLAC-LBL), p.1146.
$\eta_c'(3590)$: F. Porter *et al.*(Crystal Ball), Phys. Rev. Lett. 48 (1982) 70.
χ_c's: Ref. 38; C. J. Biddick *et al.*, Phys. Rev. Lett. 38 (1977) 1324.
45 D. Besson *et al.*(CLEO) CLNS-84/629(1984).
46 D. M. J. Lovelock *et al.*(CUSB) Phys. Rev. Lett. 54 (1985) 377.
47 L. J. Reinders, talk in session P08 of this conference.
48 K. Han *et al.*(CUSB), Phys. Rev. Lett. 55 (1985) 36.
49 S. Behrends *et al.*(CLEO), Phys. Rev. Lett. 50 (1983) 881.
50 H. Albrecht *et al.*(ARGUS) Phys. Lett. 146B (1984) 111.

51 H. Aihara *et al.*(TPC) Phys. Rev. Lett. 53 (1984) 2465.

52 Previous F meson masses above 2 GeV are obsolete. Current values are:
1970±5±5 MeV: A. Chen *et al.*(CLEO) Phys. Rev. Lett. 51 (1983) 634.
1975±9±10 MeV: M. Althoff *et al.*(TASSO) Phys. Lett. 136B (1984) 130.
1975±4 MeV: R. Bailey *et al.*(ACCMOR) PL 139B (1984) 320.
1974±3±3 MeV: H. Albrecht *et al.*(ARGUS) DESY 84-043
1963±3±3 MeV: M. Derrick *et al.*(HRS) Phys. Rev. Lett. 54 (1985) 2568.

53 D.Saxon, these proceedings.

54 D masses from review by G. Trilling, Physics Reports 75 (1981) 57.

55 B. Ratcliff (LASS), talk in session P09 of this conference.

56 e.g. M. Frank, P. J. O'Donnell, Phys. Lett. 159B (1985) 174. for a recent review see J.-M. Richard, Proc. Fifth Moriond Workshop "Heavy quarks, flavour mixing and CP violation", January 1985. See also Ref. 2.

57 H.-J. Trost (Crystal Ball), Proc. XXII Int. Conf. on High Energy Physics, Leipzig, July 1984 and SLAC-PUB-3380, DESY 84-064.

58 A. W. Nilsson (ARGUS) talk in session P08 of this conference; H. Albrecht *et al.*(ARGUS $\gamma\tau\tau$) Phys. Lett. 154B (1985) 452. H. Albrecht *et al.*(ARGUS inclusive γ) DESY 85-083. August 1985.
J. Lee-Franzini (CUSB) Proc. 5^{th} Int. Conf. on Physics in Collision, Autun, France, July 1985.
S. T. Lowe (Crystal Ball) SLAC-PUB-3683, Proc. Rencontre de Moriond, Les Arcs, March 10-17, 1985; DESY 85-042; E. D. Bloom (Crystal Ball) SLAC-PUB-3686 and Proc. 5^{th} Topical Workshop on Proton Anti-proton Collider Physics, St.Vincent, Italy, March 1985.
D. Peterson (CLEO), Proc. Int. Conf. on Hadron Spectroscopy, College Park, Maryland, April 1985.

59 F. Wilzcek, Phys. Rev. Lett. 39(1977)1304.

60 M. I. Vysotsky, Phys. Lett. 97B (1980) 159; J. Ellis, K. Enqvist, D. V. Nanopoulos, S. Ritz, CERN-TH. 4143, April 1985, and references therein.

61 for example: M. Drees, K. Grassie, Phys. Lett. 149B (1984) 367.

62 K. F. Einsweiler (Mark III), Proc. Int. Europhysics Conf. on High Energy Physics, Brighton, July 1983; D. Hitlin (Mark III), Int. Symp. on Lepton and Photon Interactions, Cornell, August 1983.

63 K. F. Einsweiler (Mark III), Ph.D. Thesis, SLAC-272, May 1984.

64 N. Wermes (Mark III), Proc. 5^{th} Int. Conf. on Physics in Collision, Autun, France. July 1985 and SLAC-PUB-3730.

65 R. M. Baltrusaitis *et al.*(Mark III), SLAC-PUB-3786, submitted to Phys. Rev. Lett. and W. Toki (Mark III), talks at 13^th SLAC Summer Institute on Particle Physics, July 1985, and Int. Symp. on Lepton and Photon Interactions at High Energies, Kyoto, August 1985.

66 B. Jean-Marie, talk in session P09 of this conference and contributed paper J. E. Augustin *et al.*, Orsay preprint LAL/85-27, July 1985; also J. E. Augustin, XX Rencontre de Moriond, Les Arcs, March 10-17, 1985 and LAL/85-17; J. E. Augustin, Proc. XXII Int. Conf. on High Energy Physics, Leipzig, July 1984.

67 P. Baillon *et al.*, Nuovo Cim. 50A (1967) 393; P. Baillon, CERN/EP 82-127, Proc. XXI Int. Conf. on High Energy Physics, Paris, 1982; P. Baillon, CERN/EP 83-82, Proc. 7^{th} Int. Conf. on Experimental Meson Spectroscopy, Brookhaven, 1983.
68 C.Dionisi *et al.*, Nucl. Phys. B169 (1980) 1.
69 T. Armstrong *et al.*(WA76), Phys. Lett. 146B (1984) 273.
70 J.Dowd (BNL-MPS), talk in session P09 of this conference.
71 S.U.Chung (BNL-MPS), Proceedings of 20th Rencontre de Moriond, Les Arcs, March 10-17, 1985 and BNL 36493; D.Zieminska (BNL-MPS), Proceedings of the International Conference on Hadron Spectroscopy, College Park, Maryland, April 1985.
72 D. L. Scharre *et al.*(Mark II), Phys. Lett. 97B (1980) 329.
73 C. Edwards *et al.*(Crystal Ball), Phys. Rev. Lett. 49 (1982) 259.
74 J.D.Richman (Mark III) Ph.D. Thesis, Caltech, CALT-68-1231 (1985); Proc. Symp. on High Energy e^+e^- Interactions, Vanderbilt, April 1984, Caltech preprint CALT-68-1136,
75 C. Edwards *et al.*(Crystal Ball), Phys. Rev. Lett. 51 (1983) 859.
76 K. Königsmann, SLAC-PUB-2910 (1980), XVII Rencontre de Moriond, Les Arcs, 1982.
77 J. J. Becker, PhD Thesis U.of Illinois; W.Toki, 11^{th} SLAC Summer Institute on Particle Physics (1983).
78 A. Billore, R. Lacaze, A. Morel, H. Navelet, Phys. Lett. 80B (1979) 381.
79 S. Berman, M. Jacob, Phys. Rev. 139B (1965) 1023.
80 S. Flatté, Phys. Lett. B63 (1976) 224; J.B.Gay *et al.* p.220.
81 R. N. Cahn and P. V. Landshoff, CERN-TH.4191/85, June 1985.
82 M. Frank, talk in session P09 of this conference, and M. Frank, N. Isgur, P. J. O'Donnell, J. Weinstein, Phys. Lett. 158B (1985) 443.
83 Ch. Zemach, Phys. Rev. 140B (1965) 97 and 109; 133B (1964) 1201.
84 S. U. Chung *et al.*(BNL-MPS), Phys. Rev. Lett. 55 (1985) 779; S.U.Chung, Proceedings of the XXII International Conference on High Energy Physics, Leipzig, July 1984, p. 167.
85 S.D.Protopopescu, Proceedings of 19th Rencontre de Moriond, La Plagne, March 4-10 (1984) 689; see also D. Reeves, Ph.D. Thesis, Florida State Univ. preprint FSU-HEP-850801, Aug. 1985.
86 N. Stanton *et al.*, Phys. Rev. Lett. 42 (1979) 346.
87 Ph. Gavillet *et al.*, Zeit. Phys. C16 (1982) 119.
88 S. I. Bitukov *et al.*(Lepton-F), Serpukhov preprint IFVE 85-19, 1985.
89 P. Chauvat *et al.*(R608), Phys. Lett. 148B (1984) 382.
90 Ph. Gavillet *et al.*, Phys. Lett. 69B (1977) 119.
91 L. Köpke, talk in session P09 of this conference and in the Proceedings, Santa Cruz preprint SCIPP 85/45.
92 (Mark III) SLAC-PUB-3435, submitted to Phys. Rev. (1985);
H. E. Haber, J. Perrier, Santa Cruz preprint SCIPP 85/39, submitted to Phys. Rev. (1985).
93 W. Bartel *et al.*(JADE), DESY 85-081, 1985.
94 M. Althoff *et al.*(TASSO), DESY 85-093, August 1985.

95 G. Gidal (Mark II), talk at 16^{th} Symp. on Multiparticle Dynamics, Kiryat-Anavim, Israel, June 1985, LBL-19992.
96 A. Ando *et al.*, contributed paper to session P09 of this conference, KEK Preprint 85-15, June 1985.
97 Th. Mouthuy (GAMS), talk in session P09 of this conference and in Proceedings.
98 T. A. Armstrong *et al.*(WA76), contributed paper to session P09 of this conference; A. Palano *et al.*(WA76), CERN/EP 83-107 (1983).
99 C. Edwards (Crystal Ball) Ph.D. thesis, Caltech, CALT-68-1165.
100 D. L. Burke *et al.*(MarkII), Phys. Rev. Lett. 49 (1982) 632.
101 R.M.Baltrusaitis *et al.*(MarkIII), SLAC-PUB-3682, May 1985, submitted to Phys. Rev. D.
102 N. Wermes (Mark III), Proc. XIXth Rencontre de Moriond, La Plagne, 1984 and SLAC-PUB-3312.
103 N. P. Chang, C. T. Nelson, Phys. Rev. Lett. 40 (1978) 1617;
T. L. Trueman, Phys. Rev. D18 (1978) 3423.
104 R.Brandelik *et al.*(TASSO), Phys. Lett. 97B(1980)448;
D.L.Burke *et al.*(MarkII), Phys. Lett. 103B(1981)153;
H.J.Behrend *et al.*(CELLO), Zeit. Phys. C21(1984)205.
105 M.Althoff *et al.*(TASSO), Zeit. Phys. C16(1982)13.
106 R.M.Baltrusaitis *et al.*(MarkIII), Phys. Rev. Lett. 55 (1985) 1723.
107 N. N. Achasov and G. N. Shestakov, Phys. Lett. 156B (1985) 434.
108 N. A. Tornqvist, Ann. Phys. 123 (1979) 1; M. Roos and N.A.T., Zeit. Phys. C5 (1980) 205.
109 C. Edwards *et al.*(Crystal Ball), Phys. Rev. Lett. 48 (1982) 458.
f polarisation: C. Edwards *et al.*, Phys. Rev. D25 (1982) 3065.
110 M. Franklin (Mark II) Stanford Ph.D. thesis. SLAC Report 254 (1982).
111 Th. Mouthuy (GAMS), talk in session P09 of this conference and in Proceedings; D. Alde *et al.*(GAMS), CERP/EP 1985 preprint, submitted to Nucl. Phys. B; F. Binon *et al.*(GAMS), Nuovo Cim. 71A (1982) 497, 78A (1983) 313, 80A (1984) 363; Lett. Nuovo Cim. 39 (1984) 41; Phys. Lett. 140B (1984) 264.
112 J. G. Körner. J. H. Kuhn, H. Schneider, Phys. Lett. 120B (1983); and with M. Krammer, Nucl. Phys. B229 (1983) 115.
113 J. F. Donoghue, talk in session P09 of this conference and in Proceedings, Univ. of Mass. preprint UMHEP-235; Proc. Int. Conf. on Hadron Spectroscopy, College Park, Maryland, April 1985, UMHEP-226; Proc. Yukon Advanced Study Institute on the Quark Structure of Matter, Aug. 1984, UMHEP-209; and with H. Gomm, Phys. Lett. 112B (1982) 409.
114 S. Ono, Orsay preprint LRTHE 82/36. Dec. 1982.
115 A. Etkin *et al.*(BNL-CCNY) Phys. Rev. Lett. 49 (1982) 1620. S. J. Lindenbaum, talk in session P09 of this conference; Proc. "Quarks, Leptons, and their Constituents", Erice 5-15 Aug., 1984 and BNL 36610; Comm. Nucl. and Particle Physics 13 No. 6 (1984) 285.
116 Booth *et al.*(WA67), paper contributed to session P09 of this conference; Proc. XXII Int. Conf. on High Energy Physics, Leipzig, 1984. Nucl. Phys.

B242 (1984) 51.
117 H. J. Lipkin, Phys. Lett. 124B (1983) 509, Nucl. Phys. B224 (1984) 147; S. J. Lindenbaum Phys. Lett. 131B (1983) 221; H.J.L. & S.J.L., Phys. Lett. 149B (1984) 407.
118 H. Gomm, Phys. Rev. D30 (1984) 1120.
119 G. Karl, W. Roberts, N. Zagury, Phys. Lett. 149B (1984) 403.
120 P. M. Fishbane, S. Meshkov, Comm. Nucl. and Particle Physics, 13 No. 6 (1984) 325.
121 A. Etkin *et al.*(BNL-CCNY), Phys. Rev. D25 (1982) 1786.
122 C. Bemporad *et al.*, Phys. Lett. 25B (1967) 380.
123 A. Browman *et al.*, Phys. Rev. Lett. 32 (1974) 1067 and 33 (1974) 1400.
124 A. Roussarie *et al.*(Mark II), Phys. Lett. 105B (1981) 304.
125 A. Weinstein *et al.*(Crystal Ball), Phys. Rev. D28 (1983) 2896.
126 K. Wacker (Crystal Ball), talk at session P09 of this conference and in Proceedings.
127 W. Bartel *et al.*(JADE), Phys. Lett. 160B (1985) 417.
128 H. Aihara *et al.*(TPC/PEP-9), UCLA-85-013. 1985.
129 H. W. Atherton *et al.*, submitted to Phys. Lett. , 1985.
130 D. Williams, talk at 6^{th} Int. Workshop on Photon-Photon Collisions, Lake Tahoe, 1984; also in Ref. 126.
131 Bellettin *et al.*, Nuovo Cim. 40A (1965) 1139.
132 Kryshkin *et al.*, JETP 30 (1970) 1037.
133 H. Kolanoski, talk at Int. Symp. on Lepton and Photon Interactions at High Energies, Kyoto, August 1985.